Chapter 5

Synthesis of carbon nanoflakes and fibrous carbon nanostructures

In this chapter, synthesis of carbon nanoflakes and fibrous nanostructures by pyrolysis in Chemical Vapour Deposition furnace from plant fibres were discussed. A total of fourteen plant fibres [Crassocephalum *(Crassocephalum crepidioides),* Palmyra *(Borassus flabellier*), Blady grass *(Imperata cylindrica),* Luffa *(Luffa cylindrica),* Pajanelia *(Pajanelia longifolia),* Daisy *(Tridax procumbens),* Eulalia *(Eualia fastigiata),* Psyllium (*Plantago* sp.), Papaya stem (*Carica papaya*), Honur (*Oroxylum indicum),* Paper flower (*Bougainvillea spectabilis),* Bontula (*Bombax insigne),* Thunga or Tak palong (*Spinacia oleracea*), Betel nut (*Areca catechu*)] were used as precursors for the production of carbon nanomaterials under catalyst free conditions. Antioxidant efficacy, photocatalytic behaviour and electrochemical behaviour of a few select synthesised materials were studied.

5.1. Introduction

As noted in the preceding chapters, carbon nanostructures have attracted much attention in the last couple of decades because of their unique structures, high electrically conductivity [1-3], and their potential applications in energy storage,

electronic, and display devices [4, 6]. Several other nanostructures have been devised, including carbon nanotubes (CNTs) and carbon nanoflakes (CNFs) [7]. Carbon nano onions, nanocapsules, single walled nanohorns and nanocones, nanospring and nano-octopus type fibers are yet another kind of carbon nanostructure that emerged recently [8-10]. The formation of these unusual carbon nano-structures is ascribed to the variation of the precursor materials and treatment parameters employed in the synthetic process [11]. Porous carbon structures have potential applications in catalysis [12-14], sensors, electronic devices, gas and liquid separation, memory storage [4-6, 15], filters, sorbents, water purification [16-19], artificial livers or kidneys [20, 21]. Carbon nano structures such as nanofibres, nanoflakes have been synthesized from a variety of nonrenewable fossil fuel based precursors such as pitch, rayon, polyacrylonitrile, acetone, hydrocarbons, solid carbon materials like artificial graphite, activated carbon, acetylene black etc. [22-27]. In keeping with the principles of green chemistry focus on variety of renewable feed stocks such as plant based oils, seeds, resins, fibrous plant tissues, lignin, cellulose etc. has been made [25, 28]. Carbon nanostructures from oil seeds such as soybeans, mustard, castor, etc. and plant based fibers such as sugar cane, baggas, coconut fibers, cellulose etc. and their capability to store hydrogen, lithium intercalation, microwave absorption, supercapacitor behaviour have been documented [29-41]. Application potential of such carbon nanofibres in the context of loading of different drug molecules aspirin, phenolphthalein, copper sulphate and anticancer drug, doxorubicin hydrochloride to act as vehicle of drug delivery to the desired sites have also been investigated [42-46]. Seeds or fibers of plants possess unique surface morphology which can be carefully preserved in carbonization process that leads to unusual nanostructures that might have potential applications in different fields.

Accordingly, in this chapter, we report the synthesis of carbon nanostructures by pyrolysis from variety of plant fibres collected from different parts of North-Eastern region. The antioxidant, photocatalytic and electrochemical behaviour of few selected materials were also studied.

5.2. Carbon nanomaterials from palmyra *(Borassus flabellier)* fibres and seeds

5.2.1. Materials

Borassus flabellifer (**Fig.5.1.)**, the Asian palmyra palm, toddy palm, or sugar palm is a robust tree and can reach a height of 30 metres. Like all *Borassus* species, it is

dioecious with male and female flowers on separate plants. The male flowers are less than 1 cm long and form semi-circular clusters, which are hidden beneath scale-like bracts within the catkin-like inflorescences. In contrast, the female flowers are golf ball-sized and solitary, sitting upon the surface of the inflorescence axis. After pollination, these blooms develop into fleshy fruits ~20 cm wide, each containing 1-3 seeds. The fruits are black to brown with sweet, fibrous pulp and each seed is enclosed within a woody endocarp. The fruits were collected from the villages of Hailakandi, Assam, India. The fibres were scrabbled up and the seeds were crushed and used as precursor to synthesize nanomaterials.

Fig.5.1. Photographs of **(a)** palmyra fruit and **(b)** palmyra fibres and **(c)** palmyra seed

5.2.2. Preparation of carbon nanomaterials

(a) Carbon nanofibres: Carbon nanofibres were produced from *Borassus flabellier* fibres by pyrolysis in a CVD furnace. The dried fibres (~10g) taken in a quartz tube was heated to 800^0C in a chemical vapour deposition furnace at a rate of 7^0C /min for 2 hours under argon flow rate of 6cm^3/min to afford a black powder. The yield recorded was 3.0 g.

(b) Carbon nanoparticles: Carbon nanoparticles were obtained from *Borassus flabellier* seed by pyrolysis. The dried and crushed seed (10g) taken in a quartz tube was heated to 800^0C in a chemical vapour deposition furnace at a rate of 7^0C /min for 2 hours under argon flow rate of 6cm^3/min to afford a black powder. The yield recorded was 2.8 g.

5.2.3. Results and discussion

The as-obtained carbon nanomaterials from both palmyra fibre and seed were black and found to be stable in air for months. The yield of carbon nanofibre was recorded to be around 30% and that of carbon nanoparticle was around 28% of initial mass.

Tap density of carbon nanofibre was calculated to be 0.27gcm^{-3} and that of carbon nanoparticles was 0.3gcm^{-3}.

5.2.3.1. Scanning electron microscopy and transmission electron microscopy

The SEM micrographs **(Fig.5.2)** of the carbon nanomaterials obtained from palmyra fibre showed the presence of millimeter long carbon nanofibres with unique surface texture. The length of the fibre is found to be more than 1.8 mm. Fibres are having some depressions on its surface at almost uniform distance apart along its length. The diameter of the shell is approximately 8µm containing clusters of beads. The beads coalesce in a particular fashion to give a flowery impression. It is noteworthy that the dimensions of the beads are in the range of sub-micrometer to a few micrometers.

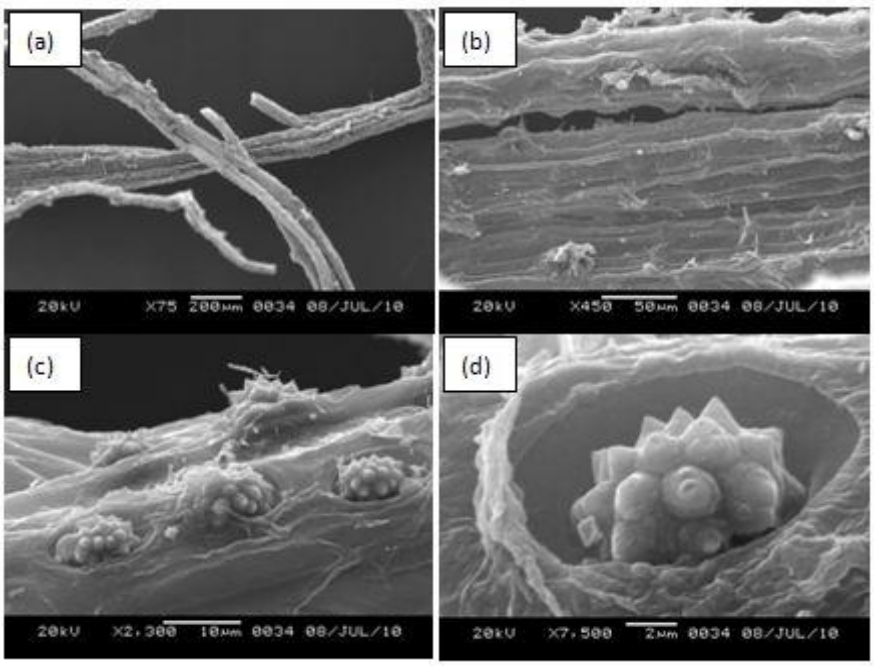

Fig.5.2.(a-d) SEM micrographs of as prepared nanofibres from palmyra fibres

The TEM micrographs (**Fig.5.3)** displayed the micrometer length spider web like nanofibres. The diameter of the fibres was found to be ~70 nm. The high resolution TEM image of the internal structure revealed the inter layer distance ~0.33 nm which resembles (002) plane of graphitic carbon. The SAED pattern showed concentric rings indicating its poly crystalline nature. It is seemed that the exceptional morphological nature can be attributed to the nature of the morphology of the plant precursor. These

unique structural features could be responsible for their profound free radical scavenging efficacy.

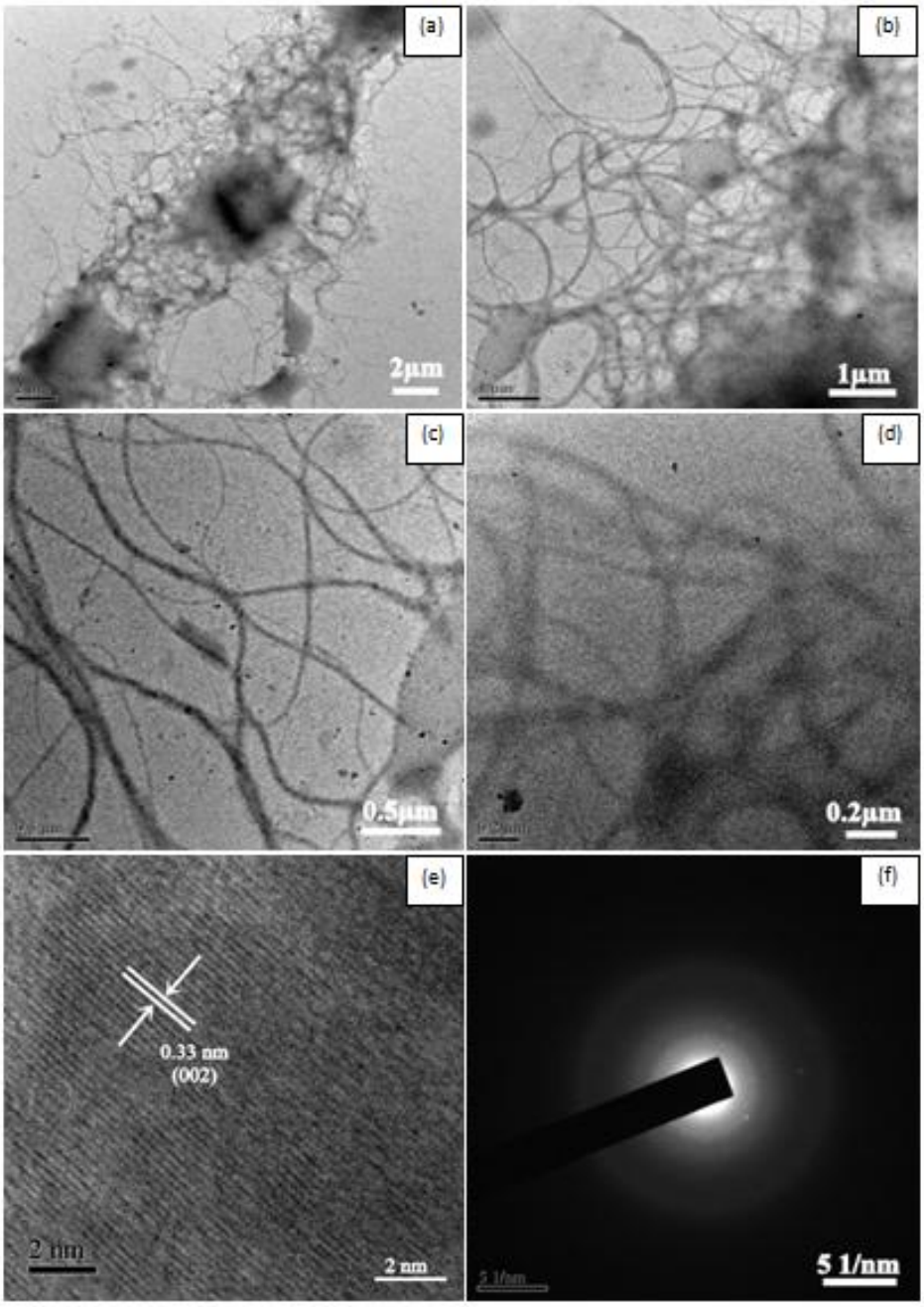

Fig.5.3. (a-d) TEM micrographs **(e)** HRTEM micrograph **(f)** SAED pattern of CNF obtained from palmyra fibre

On the other hand, the SEM micrograph **(Fig.5.4. (a))** of the nanomaterial obtained from palmyra seed showed the presence of particles. The TEM images **(Fig.5.4 (b))** indicated the presence of quasi-spherical agglomerated particle of size ~100nm. The

lattice fringes observed at interplanar distance of 0.33nm which resembles (002) plane of graphitic carbon. The SAED pattern showed concentric rings indicating graphitic ordering of the carbon.

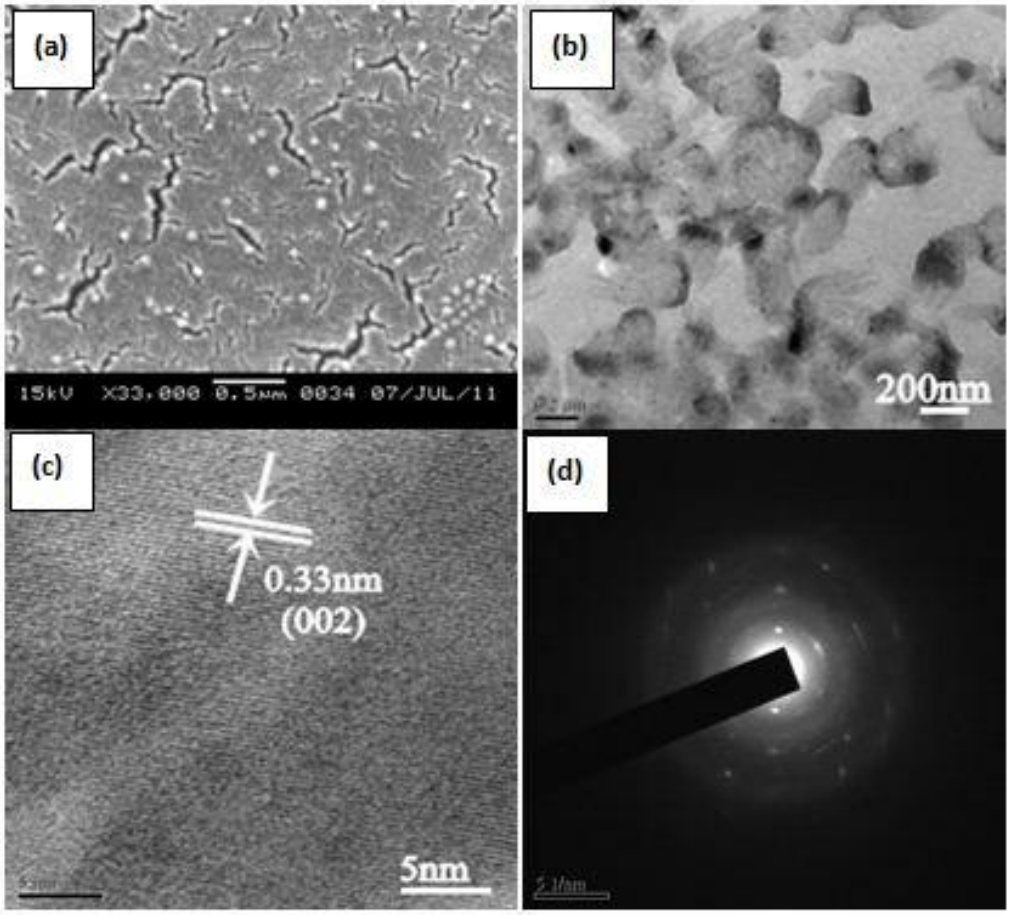

Fig.5.4. (a) SEM micrograph **(b)** TEM micrograph **(c)** HRTEM micrograph **(d)** SAED pattern of as prepared carbon nanoparticles from palmyra seeds

5.2.3.2. Powder X-ray diffraction study of carbon nanofibres

The carbon nanofibre with unique surface texture obtained from Palmyra fibres was analysed by powder X-ray diffraction. The X-ray diffraction pattern **(Fig.5.5)** showed a number of strong Bragg reflections corresponding to the (002), (100), (101), (102) (004) and (103) planes of hexagonal graphitic carbon. The average crystallite size for the most intense peak by Debye-Scherrer formula, using a Gaussian fit was found to be 21nm. Relatively sharp nature of the diffraction peaks indicates the higher degree

of graphitization. The specific surface area calculated using Sauter formula is 573.53m^2/g.

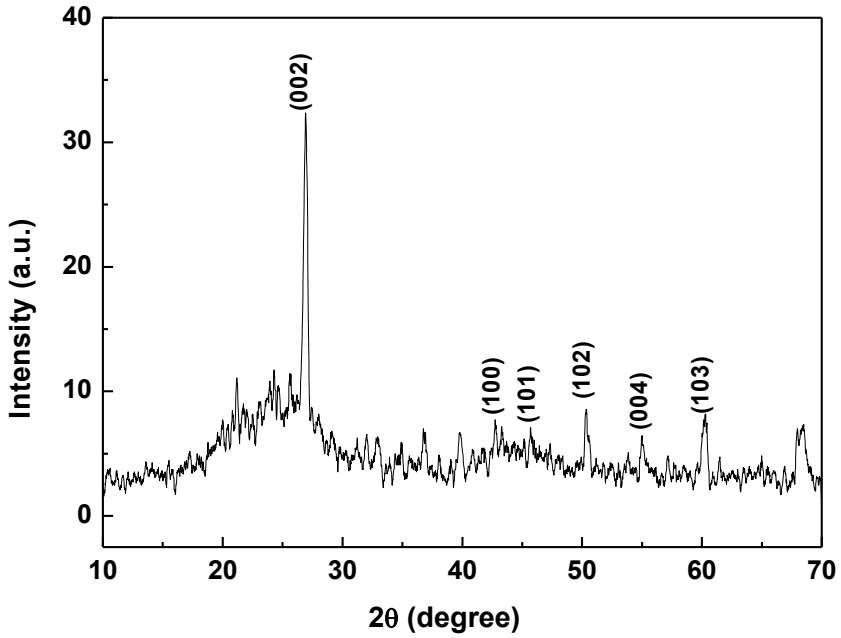

Fig.5.5. XRD of as prepared carbon nanofibres from palmyra fibres

5.2.3.3. Antioxidant activity of carbon nanofibres

The antioxidant activity of the nanofibres was assessed using a modified DPPH method for insoluble solids by UV-visible spectroscopy [47]. An amount of 4 mg powdered sample was taken in a test tube and treated with 3 mL, 100 µM methanolic solution of DPPH. To enhance the surface reaction between the nanocomposite material and the DPPH, the mixture was sonicated and kept in the dark for 15 minutes. After centrifugation at 10000 rpm, the optical absorptions of the supernatant was monitored at 517 nm. A DPPH control was also measured as reference. The aforementioned procedure was followed to ascertain time dependent DPPH scavenging at periodic interval of 15, 30, 45 and 60 minutes.The percentage scavenging was calculated using the formula,

$$\text{DPPH scavenging (\%)} = [(A_c - A_s)/A_c] \times 100$$

where A_C and A_S are absorbances of the control DPPH and DPPH with the nanocomposites at 517 nm respectively. For evaluating SC-50 (the amount of samples

required to scavenge 50% of DPPH), a similar procedure was adopted for 2, 4, 6, 8, 10 and 15 mg of the nanocomposites and absorbances recorded after 30 minutes.

The control DPPH does not show any change of absorbance with time. However, DPPH with nanomaterials showed a steady decrease of absorbance at 517nm (**Fig.5.6.(a)).**The DPPH scavenging percentage can be calculated from decline in absorbance at 517 nm, which corresponds to the quantity of DPPH in methanolic solution. It is clear from the **Fig. 5.6. (a)** that after 60 minutes more than 50% of the DPPH got scavenged for 10mg of the nanomaterials. The SC-50 value was ascertained graphically (**Fig. 5.6. (b))** and was found to be 9.5 mg. The observed antioxidant activity was attributed to the unique surface texture of the carbon nanofibres that might enhance the to the neutralization of free radical character of DPPH [48].

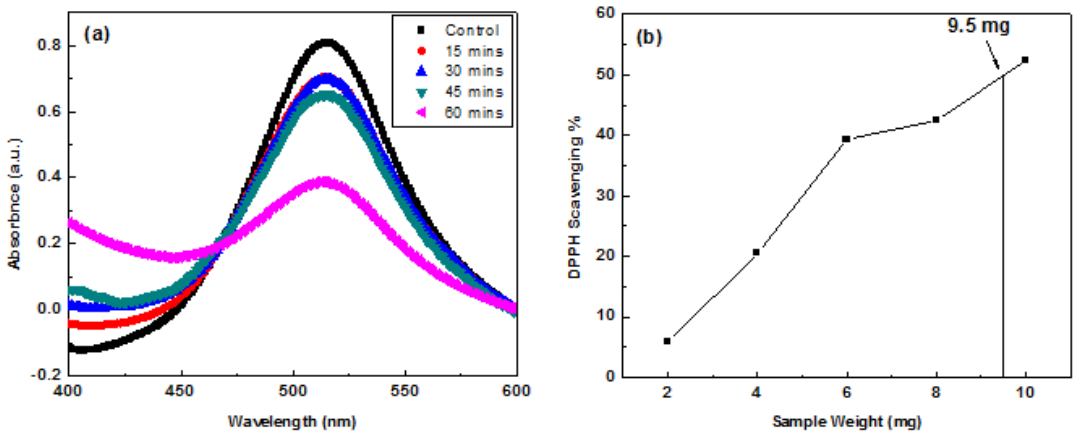

Fig.5.6. (a) DPPH radical scavenging **(b)** SC-50 value of as prepared carbon nanofibres

5.3. Carbon nanoflakes from blady grass *(Imperata cylindrica)*

5.3.1 Materials

Imperata cylindrica, commonly known as blady grass**.** The upper surface is hairy near the base of the plant while the underside is usually hairless. It is planted extensively for ground cover and soil stabilization near beach areas and other areas subject to erosion. Other uses include paper-making, thatching and weaving into mats and bags. It is used in traditional Chinese medicine**.** Inflorescence of *Imperata cylindrica* (**Fig.5.7**) were collected from hillock of Hailakandi Assam, India used as carbon precursors for the synthesis of the carbon nanoflakes.

Fig.5.7. Photo graphs of **(a)** blady grass **(b)** inflorescence of blady grass

5.3.2. Synthesis of carbon nanoflakes

Carbon nanoflake was produced from inflorescence of *Imperata cylindrica* by pyrolysis in a CVD furnace. A quartz boat loaded with the dried inflorescence (~10 g) inserted in a horizontal quartz tube is placed in the furnace. The tube was initially flushed with argon gas to eliminate air from the tube. The gas was then purged at a flow rate of 6cm^3/min. The furnace was heated to 800 ^{0}C at a rate of 7 ^{0}C min^{-1} for 2 hours to complete the process of pyrolysis. The system was then allowed to cool to room temperature under inert condition and the black powder was taken out from the quartz boat and analyzed as obtained (yield 2.8 g).

5.3.3. Results and discussion

The ‘as obtained’ material was black and found to be stable in air for months. The yield of the material was recorded to be around 28% of initial mass. Tap density of the material was calculated to be 0.22gcm^{-3}.

5.3.3.1. Scanning electron microscopy and transmission electron microscopy

The SEM micrographs **(Fig.5.8 (a,b))** of the as obtained carbon nanomaterials indicated the presence of flakes of irregular shape. The thickness of the flake was found to be in the range 37- 41 nm. The high-resolution TEM image **(Fig.5.8(c))** indicated the lattice fringes at an interplanar distance of 0.33nm which correspond to (002) plane of graphitic carbon. The defused concentric rings in SAED pattern

attested the limited graphitic ordering the carbon. The disordered texture of the carbon was further confirmed by the powder X-ray diffraction pattern.

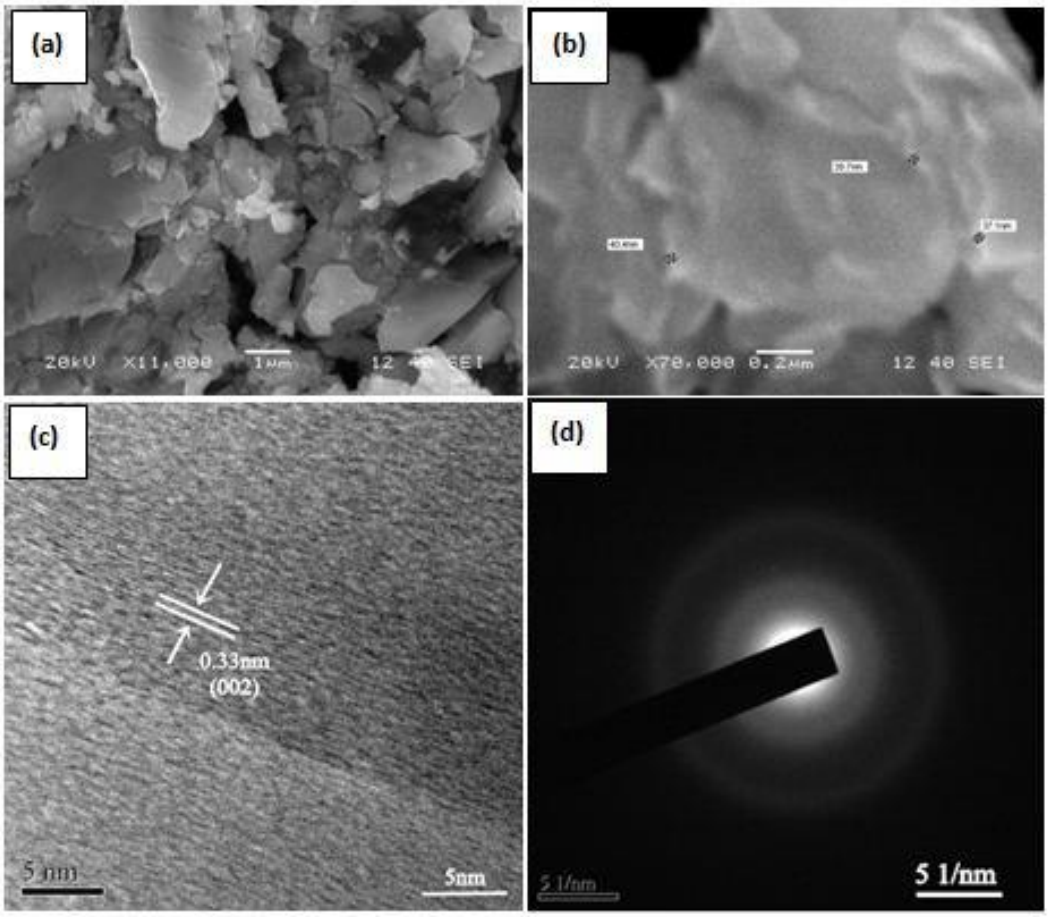

Fig.5.8. (a,b)SEM micrographs **(c)** HRTEM micrograph **(d)** SAED pattern of as prepared nanoflakes from inflorescence of *Imperata cylindrica.*

5.3.3.2. X-ray diffraction study

The powder XRD pattern of the as-obtained carbon nanoflakes **(Fig.5.9)** showed a broad peak at $2\theta = 25.5^0$ and secondary peaks at 42.9^0, $44.7^{0,}$ 50.9^0 and 60.7^0 corresponding to the (002), (100) (101), (102) and (103) planes, respectively of hexagonal graphitic carbon (JCPDS Card No. 23-0064). The broad width of the diffraction peak indicates a low degree of graphitization. The average crystallite size estimated by the Debye-Scherrer equation using a Gaussian fit was found to be 24.5 nm.

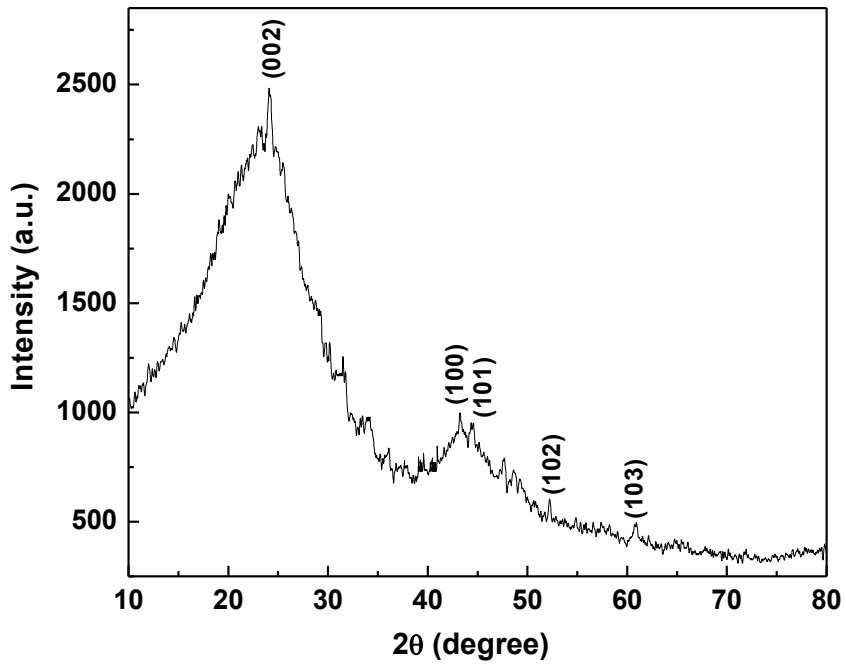

Fig.5.9. XRD pattern of the nanoflakes obtained from inflorescence of *Imperata cylindrica*

5.3.3.3. Antioxidant activity of carbon nanoflakes

The antioxidant activity of as- obtained carbon nanoflakes was measured on the basis of the scavenging activity of the stable 1, 1- diphenyl 2-picrylhyorazyl (DPPH) free radical (as described in detail in section **5.2.3.3).** For evaluating SC-50 (the amount of samples required to scavenge 50% of DPPH), 2, 4, 6, 8, 10, 15 and 20 mg of the nanoflakes were taken and absorbances were recorded at a regular interveral of time. As evident from **(Fig.5.10)** more than 60% of the DPPH were scavenged after 60 min, for 20 mg of the as-prepared carbon nanoflake. The SC-50 value was ascertained graphically to be 17.4 mg. It is pertinent here to mention that carbon nanoflakes is found to have much higher value of SC-50 than that of carbon nanofibres obtained from palmyra fibre with unique surface texture (Section **5.2.3.3.**).

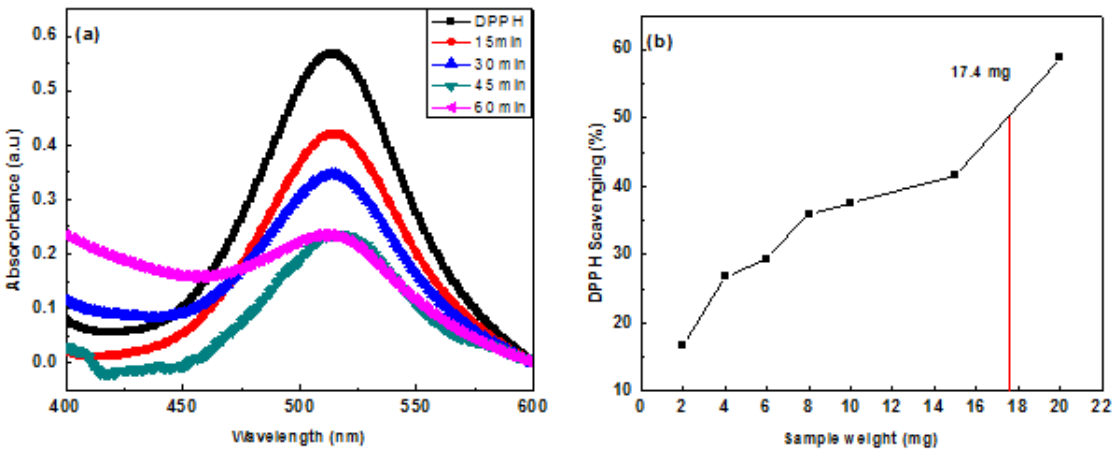

Fig.5.10. (a) DPPH radical scavenging **(b)** SC-50 value of as prepared nanoflakes

5.4. Carbon nanofibres from luffa (*Luffa cylindrica)* fibres

5.4.1. Materials

The raw materials used for the synthesis were fibres of *Luffa cylindrica,* locally called purol **(Fig.5.11)**. The plant grows wild in the bush, river bank and beach and also cultivated. The fruits of the plant are hanging or lying on the ground. The inside of the ripe fruit contained a tightly woven fibre. The extensive literature review elaborates the use of luffa in various ways from the ancient time. It has been used throughout India as a vegetative source and also as natural remedy for treatment of various degenerative disorders including inflammatory disorders and liver diseases. Its juice is used as a natural remedy for jaundice. The fibres of *Luffa cylindrica* were collected from Hailakandi, Assam, India and thoroughly washed, sun dried and used as precursor to synthesize nanofibres.

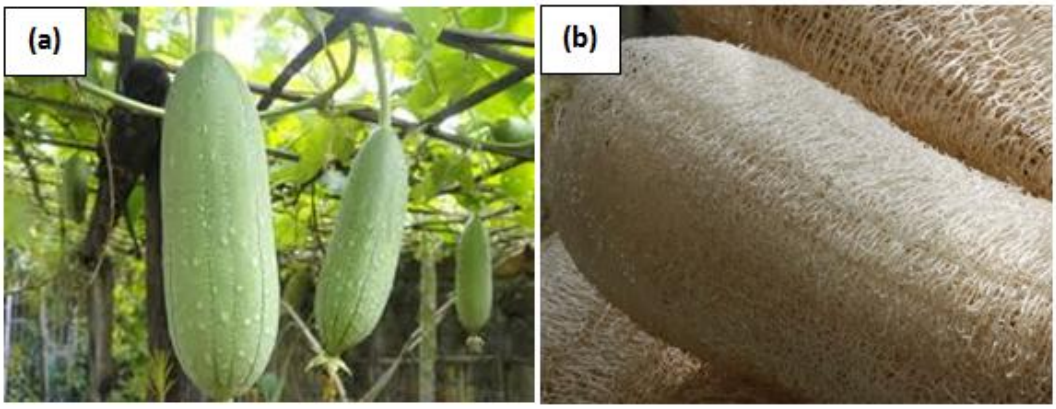

Fig.5.11. Photographs of **(a)** *Luffa cylindrica* fruit **(b)** *Luffa cylindrica* fibre

5.4.2. Synthesis of carbon nanofibres (CNF)

Carbon nanofibres were synthesized by pyrolysing luffa fibre in an inert atmosphere using CVD furnace. 10 g of the luffa fibre was taken in a quartz boat which was placed inside a quartz tube of the CVD chamber. The carrier gas argon was allowed to flow into the quartz tube with a fixed flow rate of 6 ml/min. The flow of carrier gas was maintained throughout the experiment. After 15 min of flow, furnace was switched on to reach the desired temperature 800^0C. After the completion of pyrolysis, furnace was switched off and carbon nanomaterial formed inside the quartz tube was collected and analysed as obtained. The yield was recorded to be 2.9 g.

5.4.3. Results and discussion

The as obtained black nanopowder was found to be stable in air for months and can be dispersed in aqueous and organic solvents (methanol, ethanol) under ultrasonication. The yield of the material was recorded to be around 29% of initial mass. Tap density of the material was calculated to be 0.33gcm^{-3}.

5.4.3.1. Scanning electron microscopy and transmission electron microscopy

SEM micrograph (**Fig. 5.12 (a)**) of the as obtained carbon nanofibres showed the presence of a bunch of fibres of length more than 650μm. The TEM micrographs **(Fig.5.12 (b,c))** revealed the presence of spider web like morphology of the nanofibres.

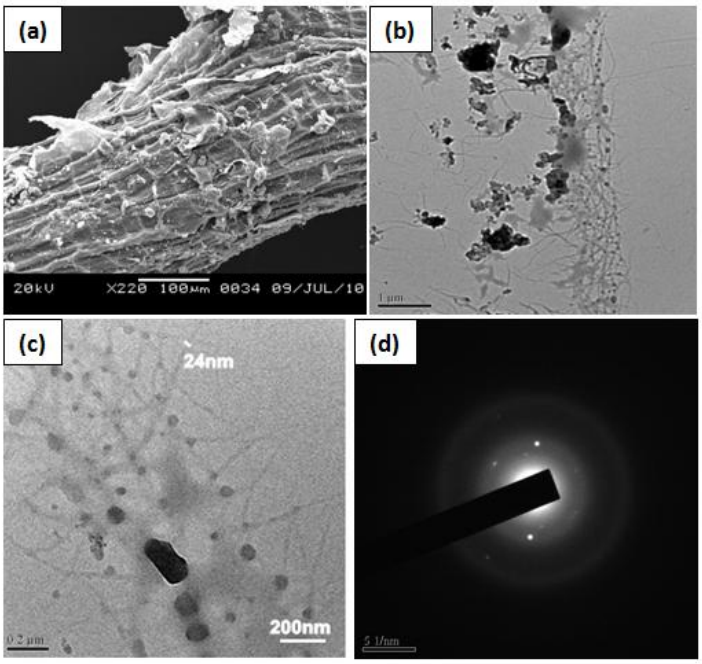

Fig.5.12. (a) SEM micrograph **(b,c)** TEM micrographs **(d)** SAED pattern of the nanofibres obtained from the fibres of *Luffa cylindrica (*Purol*)*

The diameter of the fibres was found to be ~24 nm. The selected area electron diffraction (SAED) pattern showed concentric rings indicating polycrystalline nature of the material **(Fig.5.12 (d)).** The defused nature of the rings in SAED pattern indicated the disordered texture of graphite carbon. The disordered texture was further confirmed by the powder X-ray diffraction **(Fig.5.13)** of the sample.

5.4.3.2. XRD analysis of carbon nanofibre

The powder X-ray diffraction of carbon nanofibre obtained from luffa fibre exhibited the presence of a major Bragg peak centered at 2θ ~26^0 and secondary peaks at ~43^0, ~45^0, ~50^0, ~60^0 related to the (002), (100), (101), (102) and (103) planes of hexagonal graphitic carbon (JCPDS Card No. 23-0064) respectively. The broad nature of the (002), (100) peaks reflects the disordered graphitic character.

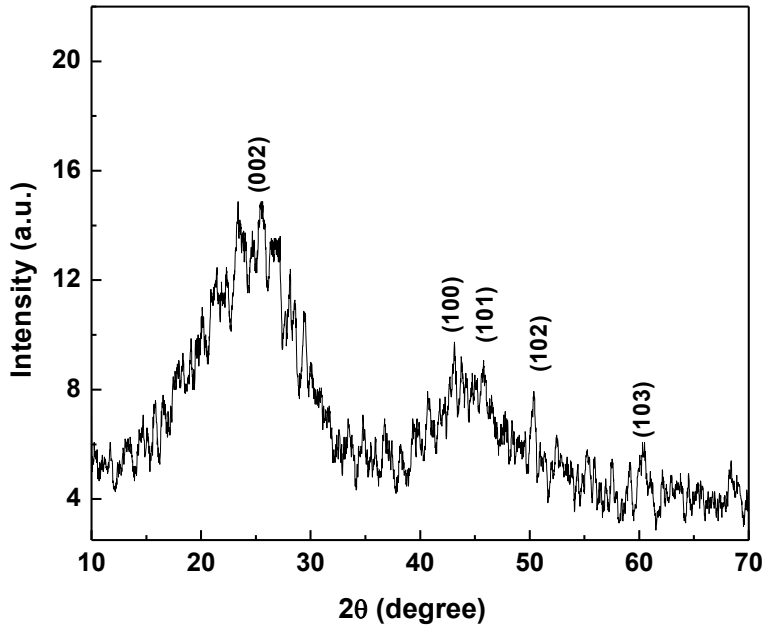

Fig.5.13. XRD pattern of the carbon nanofibres obtained from the fibres of *Luffa cylindrica*

5.5. Honey-comb carbon nanofibre from *Pajanelia longifolia* seeds

5.5.1. Materials

Pajanelia longifolia is an evergreen, or briefly deciduous, small to medium-sized, sparingly branched tree with large, ornamental flowers belongs to the family Bignoniaceae. It is found mostly on primary and secondary lowland and hill forests,

scattered along rivers and along the edges of coastal forests. The leaves, fruits, seeds and roots of plant are used for diarrhea, wounds, rheumatic arthritis and colic. The fruit of the plant were collected from Hailakandi, Assam, India and seeds were taken out, washed, sun dried and used for the synthesis of honey comb carbon nanofibre.

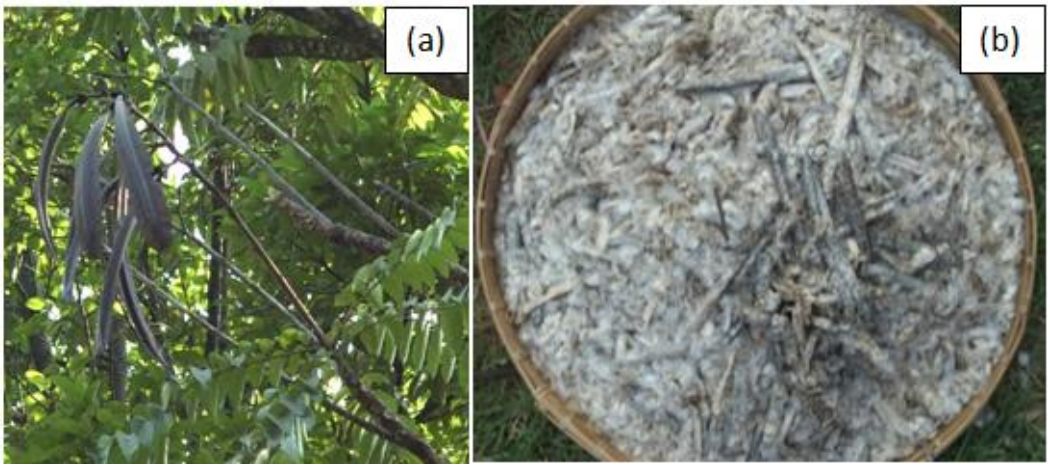

Fig.5.14. (a) *Pajanelia longifolia* plant **(b)** dried *Pajanelia longifolia* seeds

5.5.2. Synthesis of carbon nanofibre

Carbon nanofibres were synthesized by pyrolysing *Pajanelia longifolia* seeds in an inert atmosphere using CVD furnace. 10 g of the seeds was taken in a quartz boat which was placed inside a quartz tube of the CVD chamber. The carrier gas argon was allowed to flow into the quartz tube with a fixed flow rate of 6 ml/min. The flow of carrier gas was maintained throughout the experiment. After 15 min of flow, furnace was switched on to reach the desired temperature 800^0C. After the completion of pyrolysis, furnace was switched off and carbon nanomaterial formed inside the quartz tube was collected and analysed. The yield was recorded to be 2.9 g.

5.5.3. Results and discussion

The as obtained black mass was found to be stable in air for months and can be dispersed in aqueous and organic solvents (methanol, ethanol) under ultrasonication. The yield was recorded to be around 30% by weight of the initial biomass.

5.5.3.1. Scanning electron microscopy

The SEM analysis was carried out to investigate the external morphology of the as obtained carbon nanomaterials. The SEM micrographs (**Fig.5.15)** revealed the

presence of highly porous honeycomb like fibres. Pores are in the form the opening of uniform rectangular channels. Pore openings are at the mouth of the fiber and they run throughout the carbon length. The rectangular channels seemed to be stacked themselves in two dimensions keeping the third dimension constant. The pore size was found to be 7µm x 7µm. The wall thickness (pore separation) of the channel is found to be 500nm. This unique structural feature of carbon nanomaterials is of great significance in hydrogen storage, charge transport, oxygen reduction reaction and lithium ion battery [49].

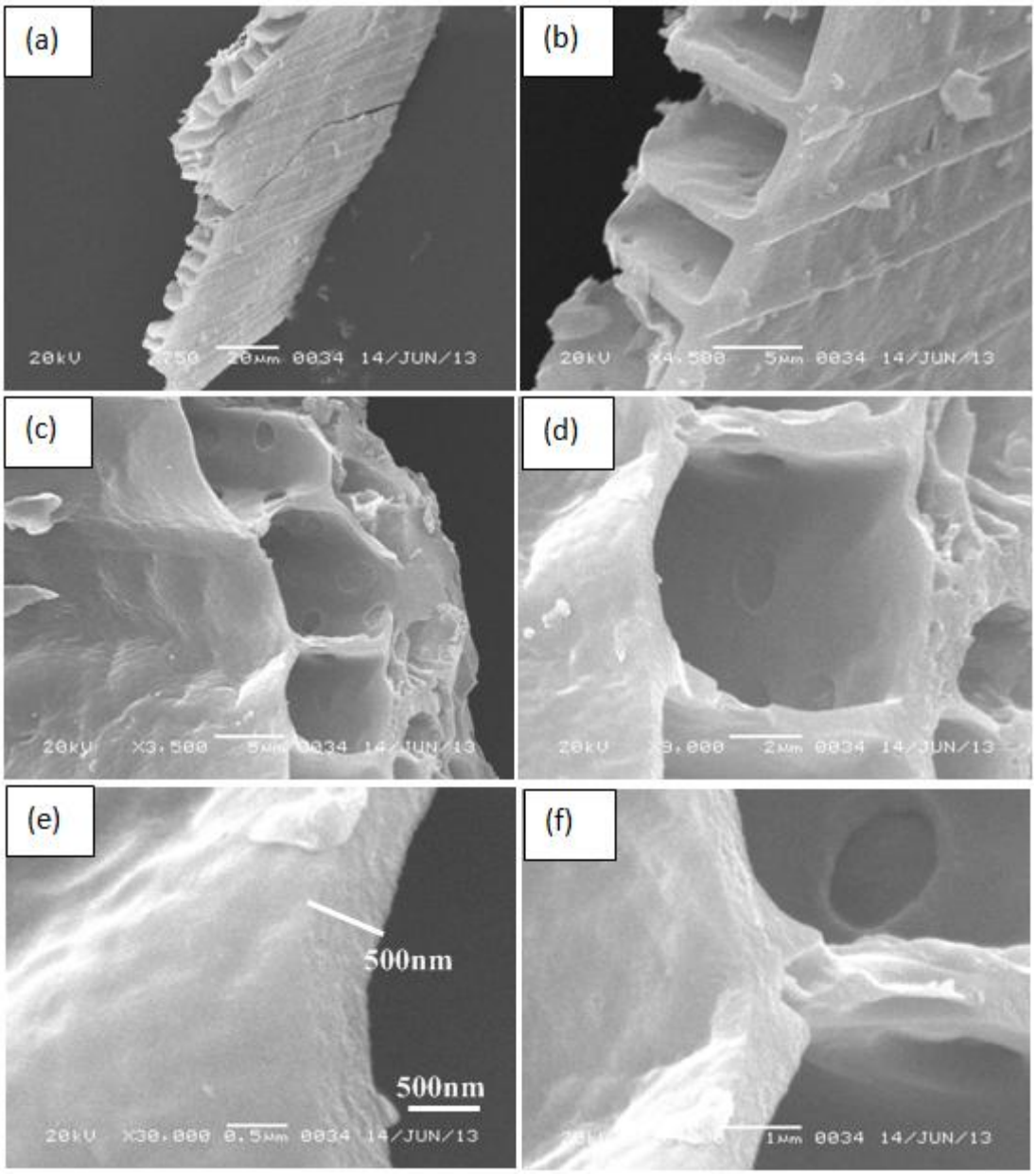

Fig.5.15. (a-f) SEM micrographs of nanofibre obtained from the seeds of *Pajanelia longifolia*

5.5.3.2. X-ray diffraction study of carbon nanofibre

The honey comb carbon nanofibres obtained from *Pajanelia longifolia* seeds were analysed by powder X-ray diffraction **(Fig.5.16).** The XRD exhibited the presence of a broad Bragg peak centered at 2θ ~26^0 corresponding to (002) plane and relatively sharp peaks at ~43^0, ~45^0, ~50^0, ~54 and ~60^0 related to the (100), (101), (102), (004) and (103) planes of hexagonal graphitic carbon (JCPDS Card No. 23-0064) respectively. The broad width and low intensity of the (002) diffraction peak indicate a low degree of graphitization.

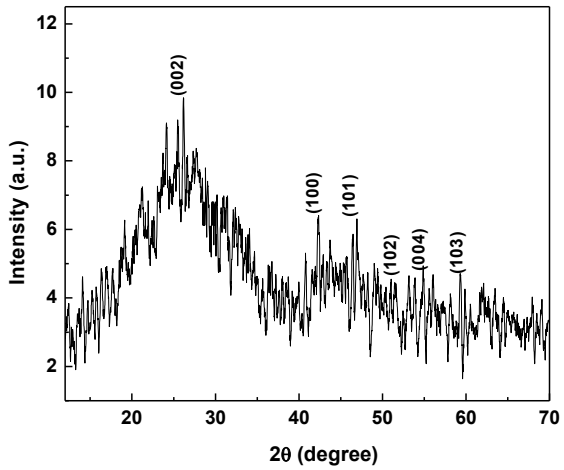

Fig.5.16. XRD pattern of nanofibre obtained from the seeds of *Pajanelia longifolia*

5.6. Carbon nanoflakes from *Crassocephalum crepidioides* seed hairs

5.6.1. Materials

Crassocephalum crepidioides commonly known as thick head is an erect annual slightly succulent herb. Its use is widespread in many tropical and subtropical regions. Its fleshy, mucilaginous leaves and stems are eaten as a vegetable, and many parts of the plant have medical uses. Seed hairs of the angiospermic plant, *Crassocephalum crepidioides* **(Fig 5.17. (a))** were collected from the S. S. College campus located in Hailakandi town, Assam, India and used as carbon precursors for the synthesis of the carbon nanoflakes. The optical micrograph of the fibrous hair is depicted in **(Fig 5.17.(b)).**

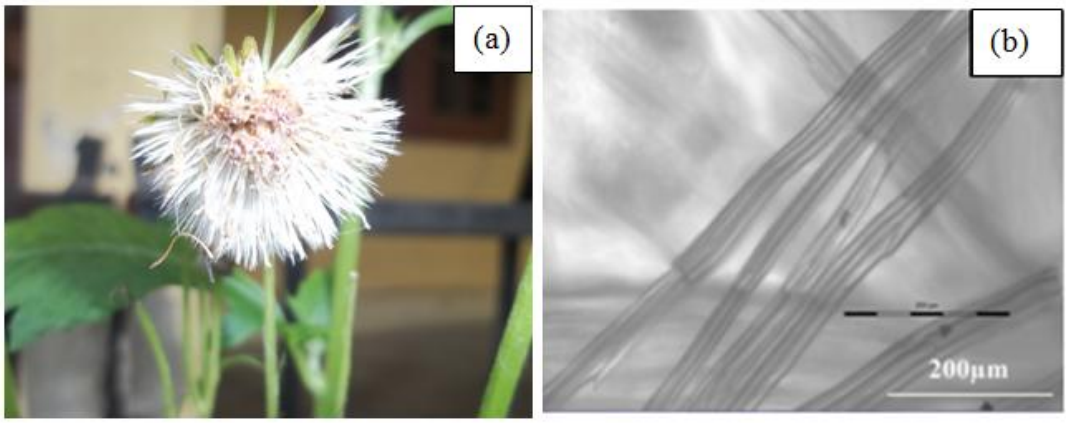

Fig. 5.17.(a) Photograph of *Crassocephalum crepidioides* plant and **(b)** optical microscopic image of seed hairs of *Crassocephalum crepidioides*

5.6.2. Preparation of carbon nanoflakes

Carbon nanoflake was produced from seed hairs of the plant, *Crassocephalum crepidioides* by pyrolysis in a CVD furnace. A quartz boat loaded with the seed hair (10 g) inserted in a horizontal quartz tube is placed in the furnace. The tube was initially flushed with argon gas to eliminate air from the tube. The gas was then purged at a flow rate of $6cm^3$/min. The furnace was heated to 800 ^{0}C at a rate of 7 ^{0}C min^{-1} for 2 hours to complete the process of pyrolysis. The system was then allowed to cool to room temperature under inert condition and the black powdered materials was collected from the quartz boat and analyzed as obtained (yield 2.5 g).

5.6.3. Results and discussion

The as obtained material was black and found to be stable in air for months. The yield of the material was recorded to be around 25% of initial mass. Tap density of the material was calculated to be $0.3gcm^{-3}$.

5.6.3.1. Transmission electron microscopy

The TEM micrographs **(Fig.5.18 (a-d))** revealed the presence of high aspect ratio nanoflakes of thicknesses less than ~10nm. The HRTEM image revealed the crystalline nature of the nanoflakes. The lattice fringes **(Fig. 5.18.(e))** were observed at an interplanar distance of 0.34 nm which correspond to (002) plane of graphitic carbon. The selected area electron diffraction (SAED) pattern **(Fig.5.18.(f))** showed concentric rings indicating polycrystalline nature of the material.

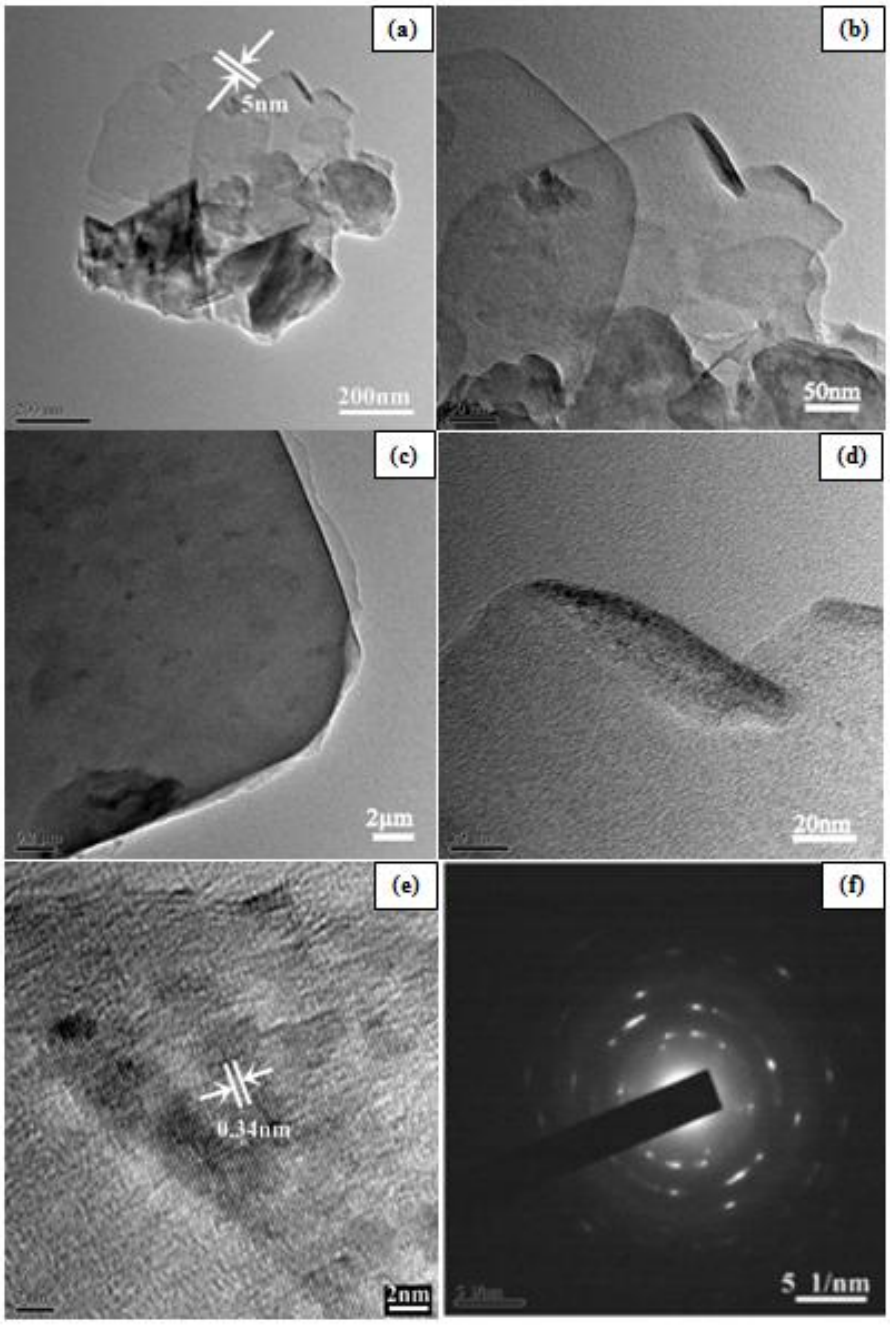

Fig. 5.18.(a- d) TEM images **(e)** HRTEM image **(f)** SAED pattern of carbon nanoflakes obtained from *Crassocephalum crepidioides* seed hairs

5.6.3.2. X-ray diffraction Study

The powder XRD pattern (**Fig.5.19.**) of as obtained nanoflakes showed two major Bragg peaks at $2\theta = 26^0$ and 42^0 along with shoulder peaks at 50^0 and 60^0 corresponding to the (002), (100), (102) and (103) planes, respectively of hexagonal graphitic carbon possessing $P6_3/mmc$ space group (JCPDS Card No. 23-0064). The broad nature of the peak suggests a lesser long range structural order. The average

crystallite size estimated by the Debye-Scherrer equation using a Gaussian fit was found to be 36nm. Specific surface area(S) calculated by using Sauter formula, $S = 6000/D \times \rho$ [50,51] is found to be 573.53 m^2/g.

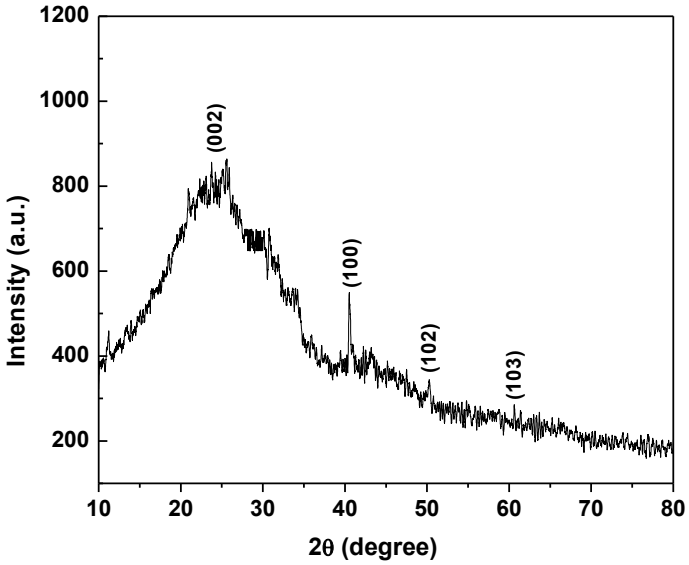

Fig.5.19. X-Ray diffraction spectrum of the carbon nanoflakes obtained from *Crassocephalum crepidioides* seed hairs.

5.6.3.3. Photocatalytic activity

Graphene, due to its unique planar structure, excellent transparency, superior electron conductivity and mobility, high specific surface area, and high chemical stability shows remarkable application in photocatalysis, including nonselective processes for degradation of pollutants, selective transformations for organic synthesis and water splitting to clean hydrogen energy [52]. Carbon nanoflakes, being structurally similar to graphene, are expected to show photo catalytic behaviour.

The photocatalytic activity of the material was evaluated by degradation of methylene blue (MB) solution under visible light irradiation. The decreasing concentration of the MB solution in the photocatalytic reaction was used to determine the effectiveness of the material as catalyst [53,54]. The intensity of the 665 nm peak of MB solution was monitored to assess the concentration of the MB in solution. A 1mg, 5mg, 10mg and 15mg of as-obtained nanoflakes as photocatalyst were added into 50 mL of MB solution in distilled water of concentrations $1x10^{-5}$ mol/L, $5x10^{-5}$ mol/L and $1x10^{-4}$ mol/L, respectively. After being dispersed in an ultrasonic

bath for 5 min, the solutions were stirred for 2 hour in the dark to reach adsorption equilibrium between the catalyst and the solution and then exposed to visible-light irradiation. The samples are taken out at specific time interval and centrifuged to separate any suspended particle. The readings are taken in a spectrophotometer at an interval of 30, 60, 90, 120, 150, 180 and 210 minutes (**Fig 5.20.(a,b)**). It is evident that the nanoflakes do not exhibit any remarkable degradation behavior in absence of light while in presence of visible-light, marked degradation was noticed (**Fig.5.20.(c)**).

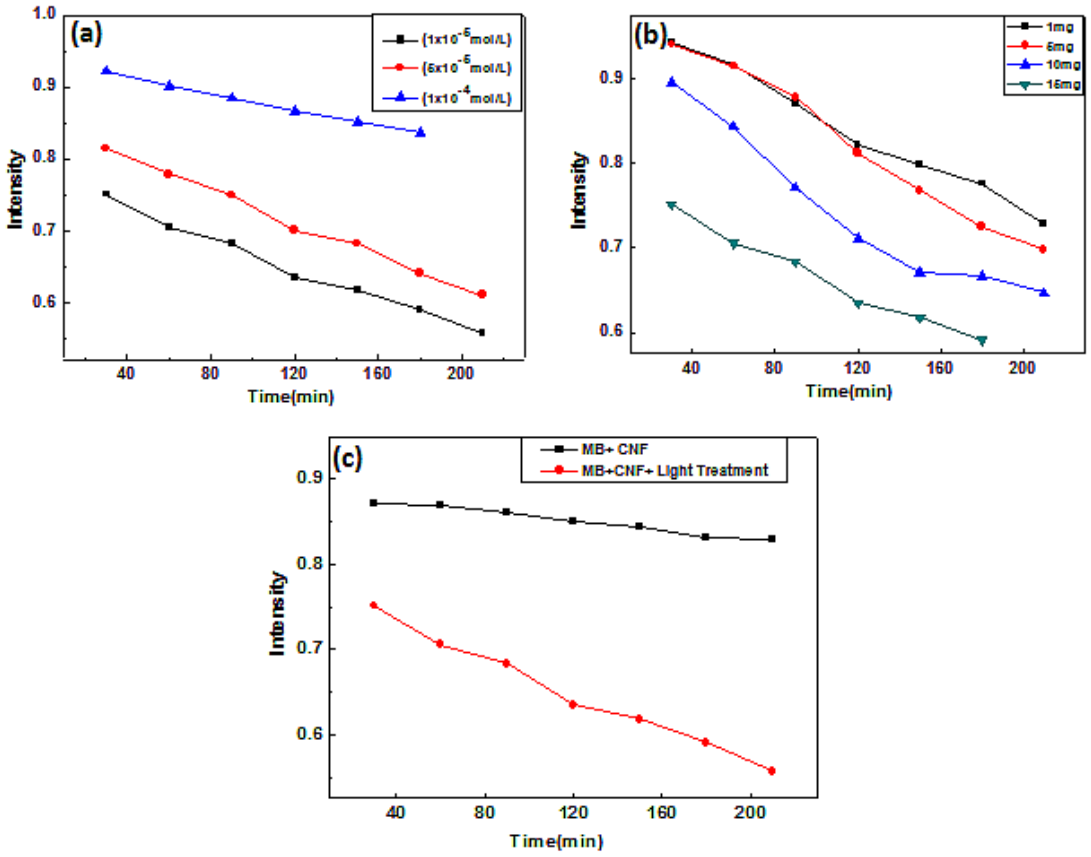

Fig. 5.20.(a) Time dependent UV-visible peak intensities at 665 nm of different concentrations of MB solution **(b)** concentration dependent UV-visible intensities at 665 nm of ($1x10^{-5}$ mol/L) with different amounts of nanoflakes material and **(c)** degradation of MB solution ($1x10^{-5}$ mol/L) with visible light treated product and non treated product (MB+CNF).

5.7. Carbon nanofibres from Daisy *(Tridax procumbens)* seed hairs

5.7.1. Materials

Tridax procumbens, commonly known as coat buttons or daisy, is a species of flowering plant in the daisy family. The plant bears daisylike yellow-centered white or yellow flowers with three-toothed ray florets. *Tridax procumbens* is known for several potential therapeutic activities like antiviral, anti oxidant antibiotic efficacies, wound healing activity, insecticidal and anti-inflammatory activity. The seed hairs of *Tridax procumbens* **(Fig.5.21)**, were collected from premises of NSNRC, Jambul phata, Maharashtra, India and thoroughly washed, sun dried and used as precursor to synthesize nanofibres.

Fig.5.21. Photograph of daisy plant

5.7.2. Synthesis of carbon nanofibres from daisy plant

Carbon nanofibres were synthesized by pyrolysing daisy seed hairs in an inert atmosphere using CVD furnace. 10 g of the seed hairs was taken in a quartz boat that was placed inside a quartz tube of CVD chamber. The argon gas was allowed to flow into the quartz tube with a flow rate of 6 ml/min. The flow of argon gas was maintained throughout the experiment. After 15 min of flow, furnace was switched on to reach the desired temperature 800^0C. After the completion of pyrolysis, furnace was switched off and carbon nanomaterial formed inside the quartz tube was collected and analysed as obtained. The yield was recorded to be 2.4 g.

5.7.3. Results and discussion

The as-obtained carbon nanofibre black powder is air stable for months and can be dispersed in aqueous and organic solvents (methanol, ethanol) under ultrasonication.

The yield of the nanomaterial was found to be around 25% by weight of the initial biomass. The tap density of the material was calculated to be 0.28gcm^{-3}.

5.7.3.1. Scanning electron microscopy and transmission electron microscopy

The scanning electron microscopy (SEM) images **(Fig.5.22 (a,b)** indicated micrometric fibres with unique textural characteristics. The surface of the fibre is well decorated with evenly spaced interconnected beads. It is noteworthy that the dimensions of the beads are in the range of sub-micrometer to a few micrometers. From the high-resolution transmission electron microscopy image **(Fig.5.22(c))**, it is observed that the material has a well defined lattice fringes. The interplanar distance is found to be 0.33nm which corresponds to (002) plane of graphitic carbon. The concentric ring pattern in SAED attested the graphitic nature of the material **(Fig.5.22(d)).**

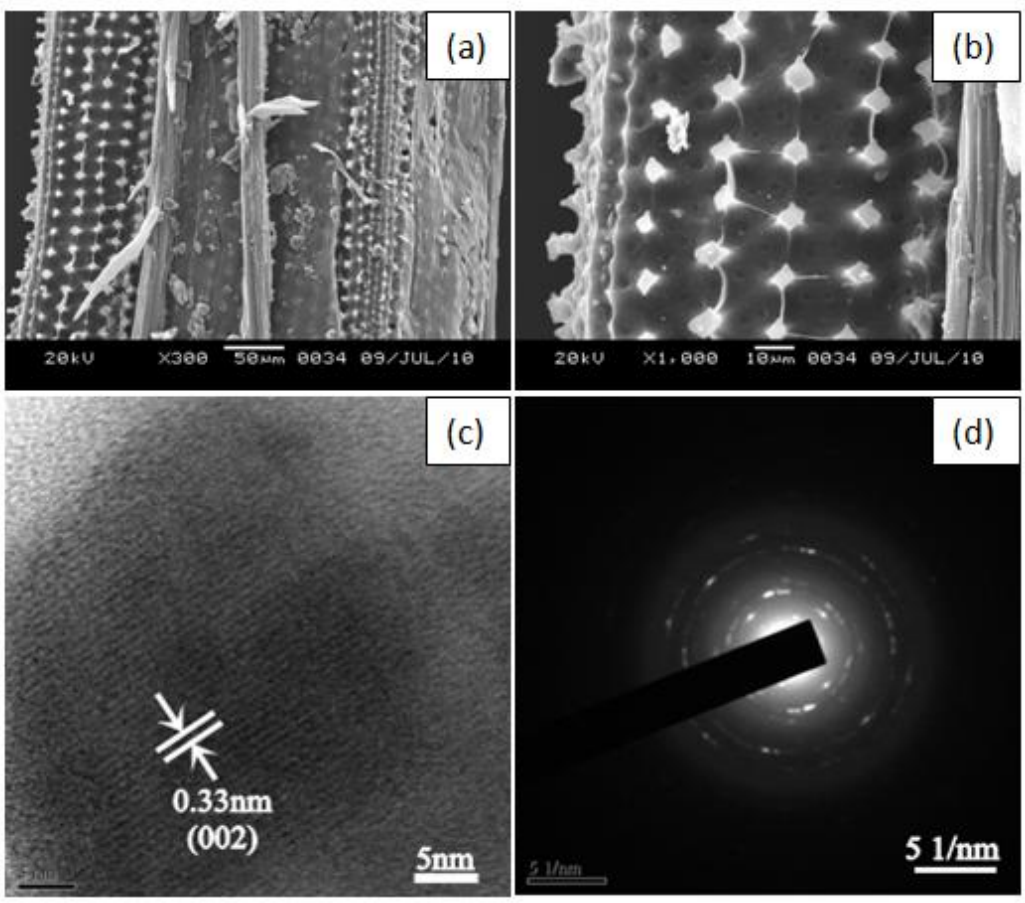

Fig.5.22.(a, b)SEM micrograph **(c)** HRTEM micrograph **(d)** SAED pattern of the nanofibres obtained from daisy seeds

5.7.3.2. XRD analysis of carbon nanofibre

The carbon nanofibres obtained from *Tridax procumbens* seed hairs were analysed by powder X-ray diffraction **(Fig.5.23).** The pattern exhibited the presence of a broad Bragg peak centered at 2θ ~26^0 corresponding to (002) plane and relatively sharp peaks at ~42^0, ~44^0, ~50^0 , ~54 and ~60^0 related to the (100), (101), (102),(004) and (103) planes of hexagonal graphitic carbon (JCPDS Card No. 23-0064) respectively. The broad width of the characteristic (002) diffraction peak indicates a low degree of graphitization.

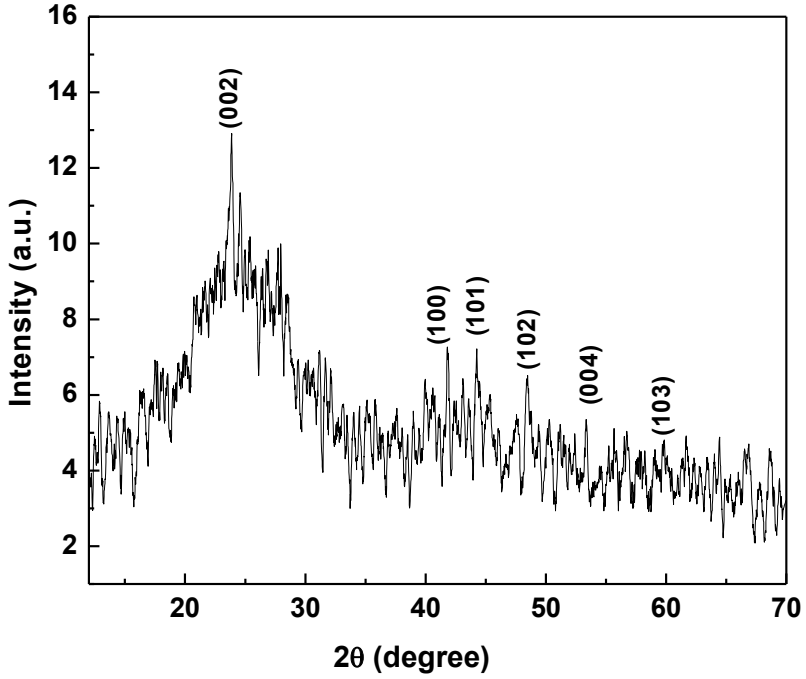

Fig.5.23. XRD pattern of the nanofibres obtained from daisy seed hair

5.8. Hollow carbon nanofibres accessed from inflorescence of *Eulalia fastigiata*

5.8.1. Materials

The matured inflorescence from rachis of *Eulalia fastigiata* was collected from the Hilly areas of north eastern region of India during December and January. The biomass was thoroughly washed, sun dried and used as precursor to synthesize carbon nanomaterials.

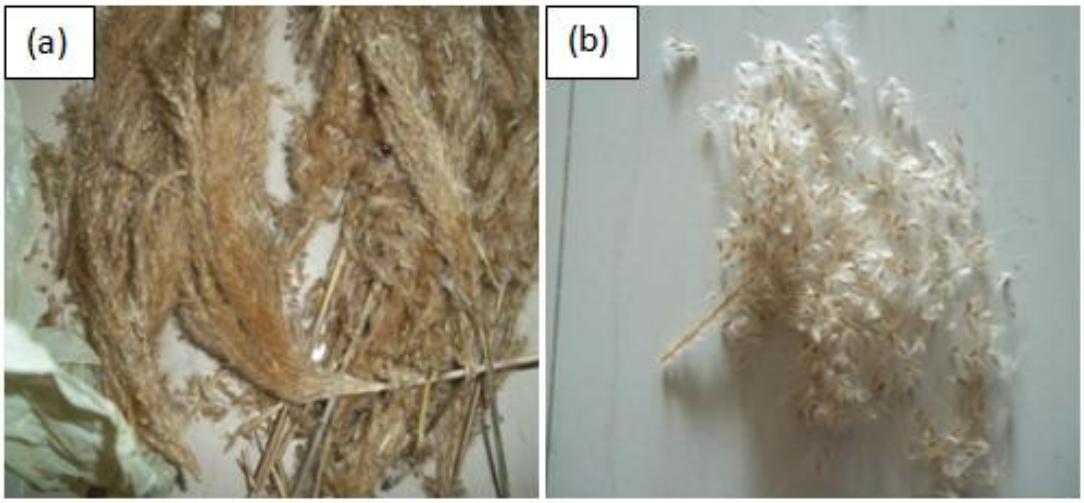

Fig.5.24. Photographs of **(a, b)** inflorescence of *Eulalia fastigiata*

5.8.2. Synthesis of carbon nanofibres

Hollow carbon nanofibres were produced from the washed and dried inflorescence of *Eulalia fastigiata* by pyrolysis in a CVD furnace. A quartz boat loaded with the precursor (10g) inserted in a horizontal quartz tube was placed in the furnace. The tube was initially flushed with argon gas in order to eliminate air from the tube and then purged at a flow rate of 6cm^3/min. The furnace was heated to 800 ^{0}C at a rate of 7 ^{0}C per minute for 2 hours to complete the process of pyrolysis. The system was then allowed to cool to room temperature under inert condition and the black powder so formed were taken out from the quartz boat and analyzed as obtained (yield 3.2 g).

5.8.3. Results and discussion

The as-obtained carbon nanofibres black powder is found to be stable in air for months and can be dispersed in aqueous and organic solvents (methanol, ethanol) under ultrasonication. The yield of the nanomaterial was found to be around ~30% by weight of the initial biomass. The tap density of the synthesised hollow carbon nanofibres was found to be 0.23g/cm^3.

5.8.3.1. Scanning electron microscopy and transmission electron microscopy

The SEM micrographs revealed the presence of uniform hollow fibres. The length of the fibres is in the range of 0.3- 1 millimeter. The outer and inner diameters are found to be ~ 8µm and 6µm, respectively.

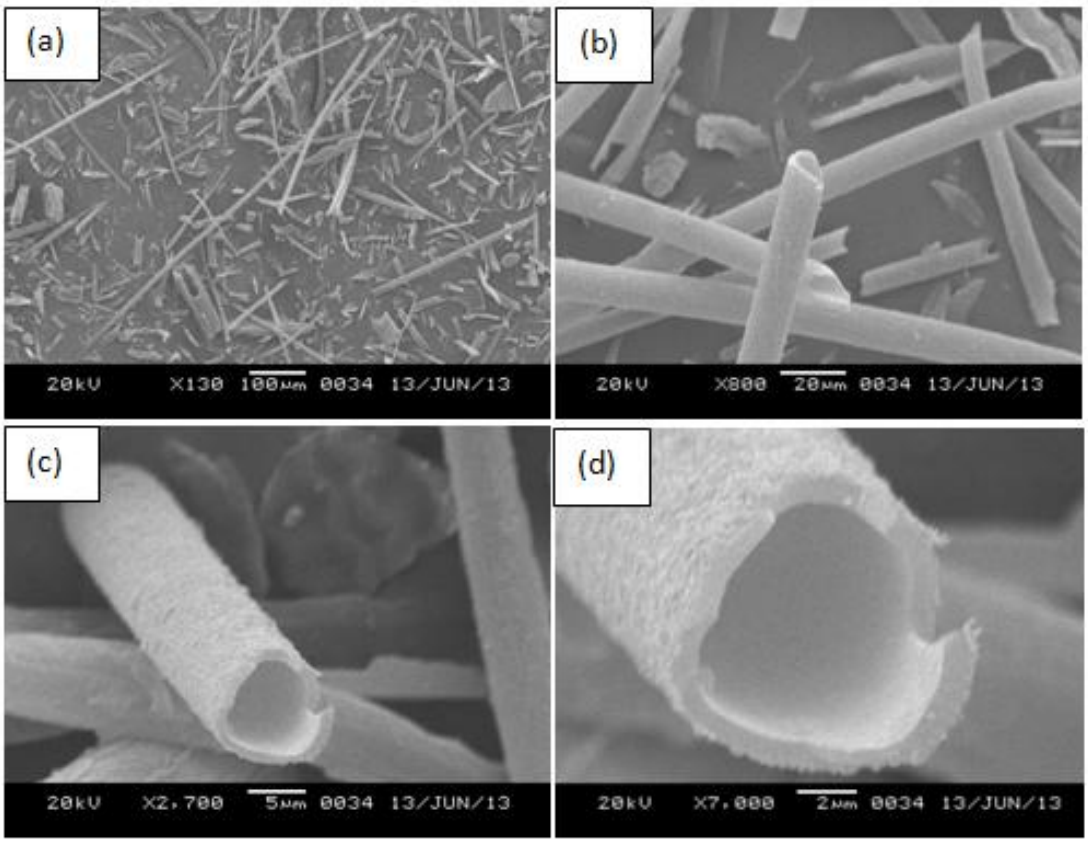

Fig.5.25. (a-d) SEM micrographs of hollow nanofibres accessed from inflorescence of *Eulalia fastigiata*

The TEM micrographs (**Fig.5.26 (a, b))** revealed that the wall of the hollow fibre consisting of graphene like sheets which rolled concentrically to form the fibre. The thickness of the sheets was found to be ~ 1nm. From high-resolution TEM image (**Fig.5.26 (c))**, the lattice fringes were observed at an interplanar distance of 0.33 nm which corresponds to (002) plane of graphitic carbon. The concentric ring pattern (**Fig.5.26 (d))** in SAED further attested the graphitic nature of the material.

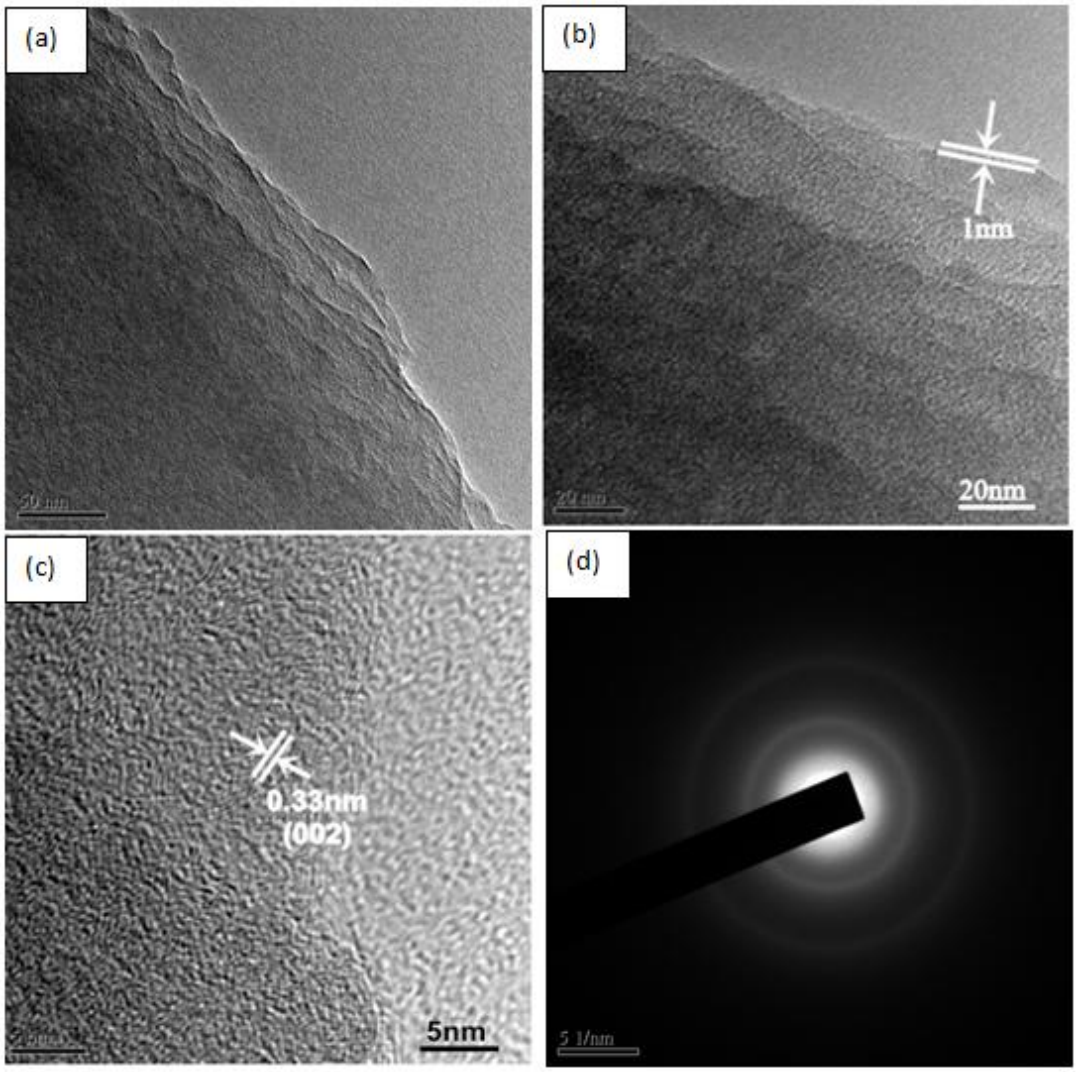

Fig.5.26. (a,b) TEM images **(c)** HRTEM image **(d)** SAED pattern of hollow nanofibres accessed from inflorescence of *Eulalia fastigiata*

5.8.3.2. X-ray diffraction study analysis of hollow carbon nanofibres

The powder XRD pattern of the as-obtained carbon nanofibres **(Fig.5.27)** showed a broad peak at $2\theta = 25.3^0$ corresponding to the (002) plane and two high intensity sharp peaks at $2\theta = 43.6^0$ and 50.9^0 corresponding to the (101) and (102) planes respectively of hexagonal graphitic carbon possessing $P6_3/mmc$ space group (JCPDS Card No. 23-0064). The broad nature of (002) peak suggests a lesser long range structural order. Interlayer spacing (d=0.33 nm) obtained from TEM and a similar value extracted from Bragg's equation evidences a rather high degree of graphitic character of carbon nanofibre.

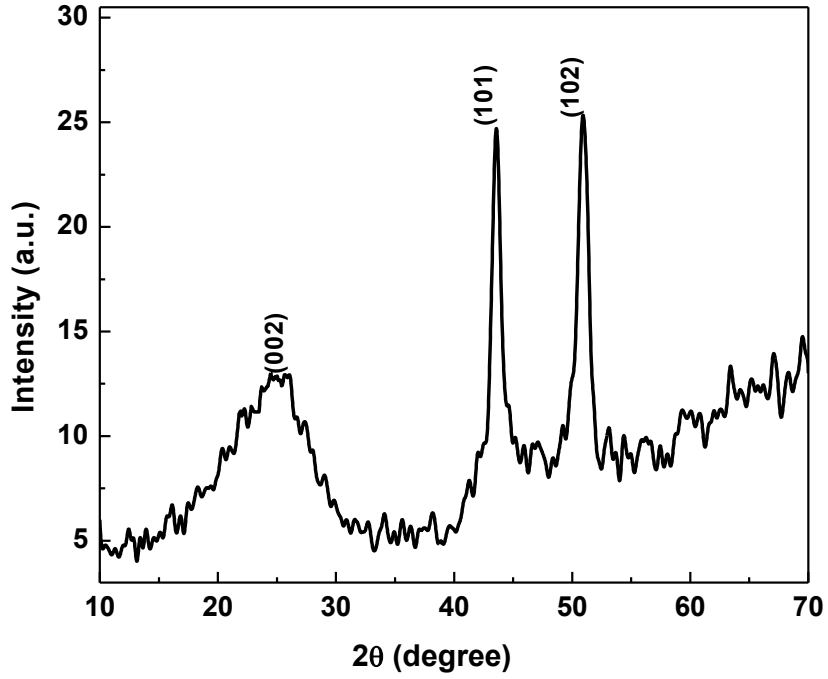

Fig.5.27. XRD pattern of nano fibres accessed from inflorescence of *Eulalia fastigiata*

5.9. Porous carbon nanomaterials from psyllium seed husk, *Plantago* sp.

5.9.1. Materials

Psyllium seed husks, also known as ishabgul are portions of the seeds of the plant *Plantago ovate*, a native of India, Bangladesh and Pakistan. They are hygroscopic, which allows them to expand and become mucilaginous. Psyllium seed husks are indigestible and are a source of soluble dietary fiber. They are used to relieve constipation, irritable bowel syndrome, and diarrhea. Ayurveda recommends its use for colon cleansing/ bowel regulation as well as for better blood circulation. They are also used as a regular dietary supplement to improve and maintain regular gastro intestinal transit. The inert bulk of the husks help to provide a constant volume of solid material irrespective of other aspects of the diet or any disease condition of the gut. These are also effective in lowering cholesterol and controlling certain types of diabetes. Other uses include gluten-free baking, where ground psyllium seed husks bind moisture and help to make breads less crumbly. The seed husks were collected,

thoroughly washed, sun dried and used as a precursor for the synthesis of nanomaterials.

Fig.5.28. Photographs of **(a)** psyllium plant **(b)** psyllium seeds and **(c)** seed husks

5.9.2 Synthesis of porous carbon nanomaterials

Porous carbon nanomaterials were produced from the washed and dried seed husk of *Plantago ovate* by pyrolysis in a CVD furnace. A quartz boat loaded with the precursor (~10 g) inserted in a horizontal quartz tube was placed in the furnace. The tube was initially flushed with argon gas in order to eliminate air from the tube and then purged at a flow rate of 6cm^3/min. The furnace was heated to 800 ^{0}C at a rate of 7 ^{0}C per minute for 2 hours to complete the process of pyrolysis. The system was then allowed to cool to room temperature under inert condition and the black powder so formed were taken out from the quartz boat and analyzed as obtained (yield 2.4 g).

5.9.3. Results and discussion

The as-obtained porous carbon nanomaterials black powder is found to be stable in air for months and can be dispersed in aqueous and organic solvents (methanol, ethanol) under ultrasonication. The yield of the nanomaterial was found to be around ~25% by weight of the initial biomass. The tap density of the synthesised porous carbon nanofibres was found to be 0.47g/cm^3.

5.9.3.1. Scanning electron microscopy

The SEM micrographs of the as obtained carbon nanomaterials were presented in **Fig.5.29.** The images indicated unique morphology**.** The porous carbon nanomaterials resembling skull-feature with disorganized micrometric cavities. It is worth mentioning that the interconnected cavities in the porous texture may serve as reservoirs for electrolyte and therefore reduce the diffusion distances of charges to the interior. Such unique textural characteristic is of great significance for fast charge transport and superior to the solid structure without space inside [55].

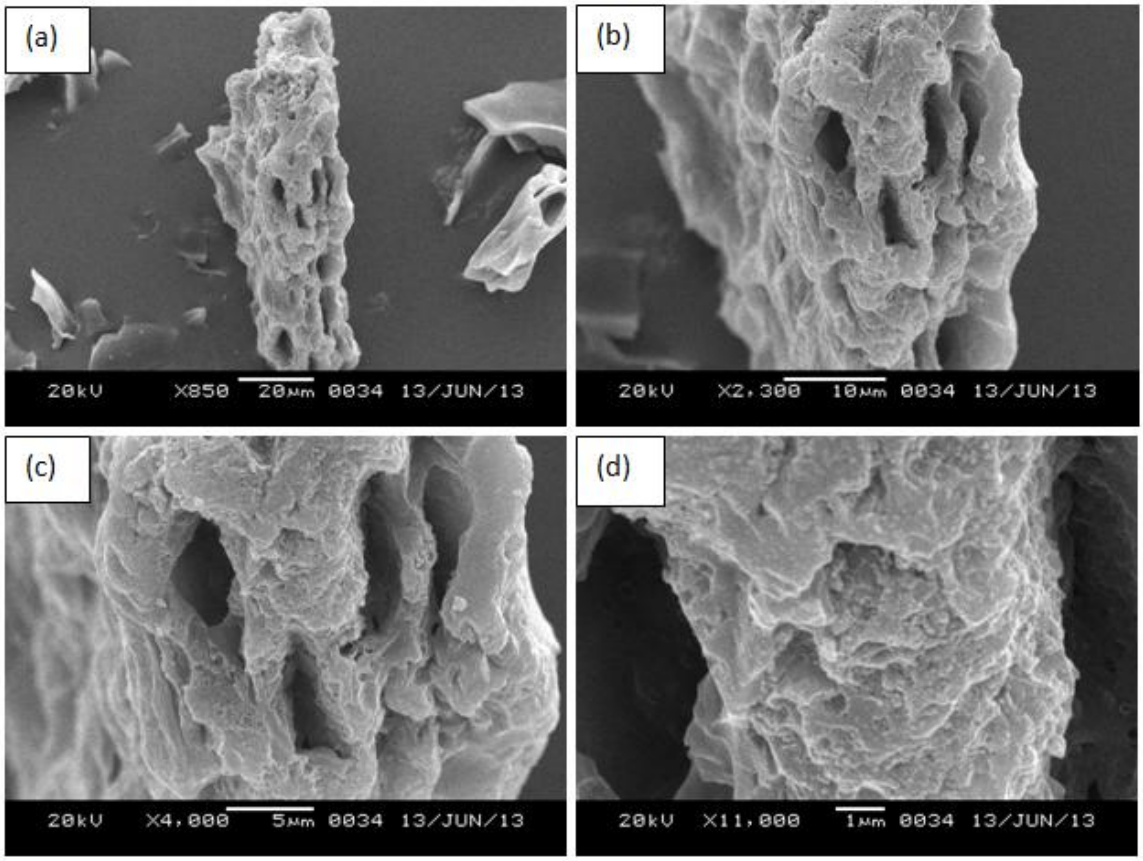

Fig.5.29.(a-d) SEM micrographs of porous carbon nanomaterials from psyllium seed husk

The TEM micrographs **(Fig.5.30)** indicated the presence of nanoflakes. The lattice fringes were not very distinct. The interplanar distance is however, calculated to be 0.33 nm which correspond to (002) plane of graphitic carbon. The defused concentric rings in SAED pattern attested the limited graphitic ordering the carbon.

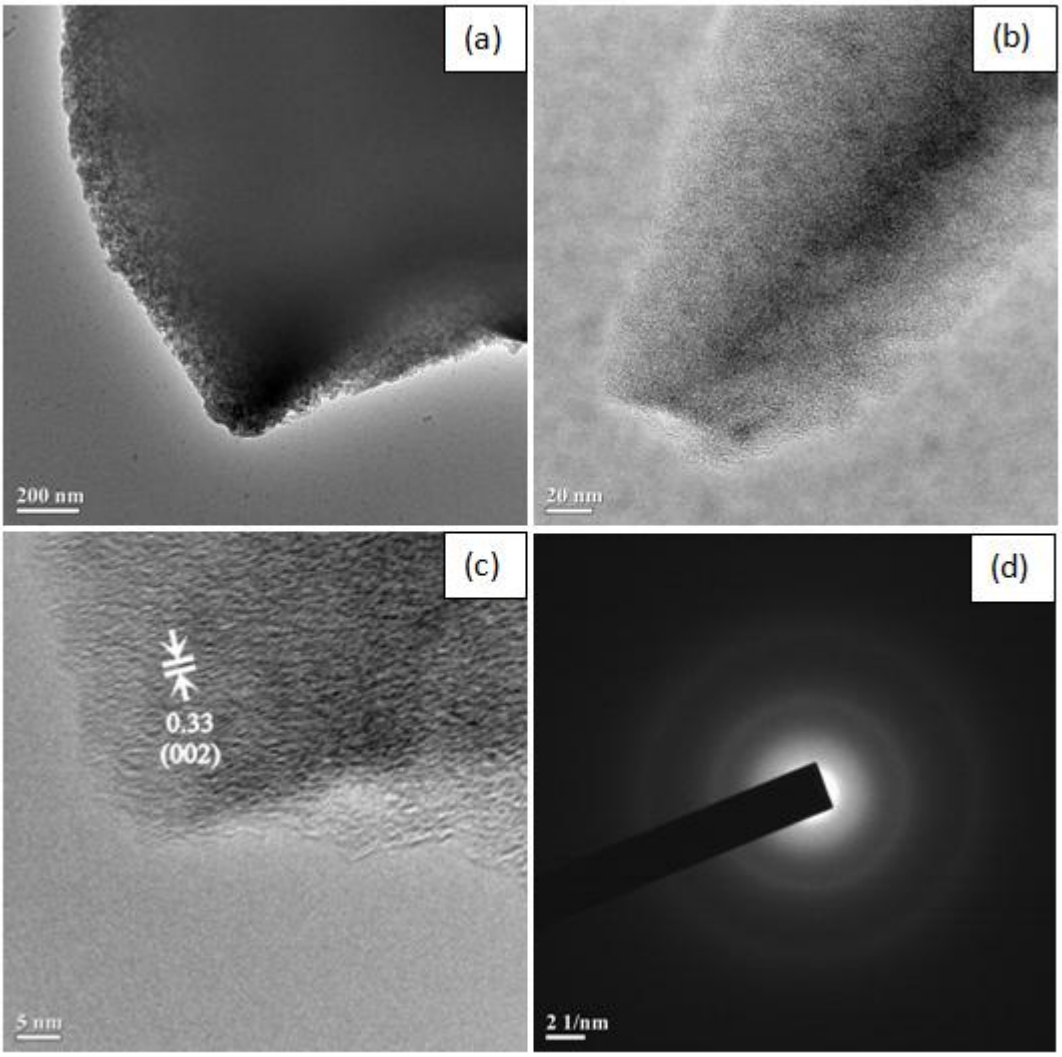

Fig.5.30.(a,b)TEM micrographs **(c)** HRTEM micrograph **(d)** SAED pattern of the porous carbon nanomaterials from psyllium seed husk

5.9.3.2. X-ray diffraction analysis

The powder XRD pattern **(Fig.5.31)** of the as-obtained carbon nanofibres showed broad peaks at 2θ = 24.02, 43.24 and 44.23 and a low intensity peak at 60.9 corresponding to the (002), (100) , (101) and (103) planes, respectively of hexagonal graphitic carbon (JCPDS Card No. 23-0064). The un- indexed peak may be due to impurity present in the sample as the material is derived from plant based precursor. The broad width of the diffraction peaks indicate a low degree of graphitization as also evidenced by TEM micrographs **(Fig.5.30)**. The average crystallite size estimated by the Debye–Scherrer equation using a Gaussian fit was found to be 12.6 nm.

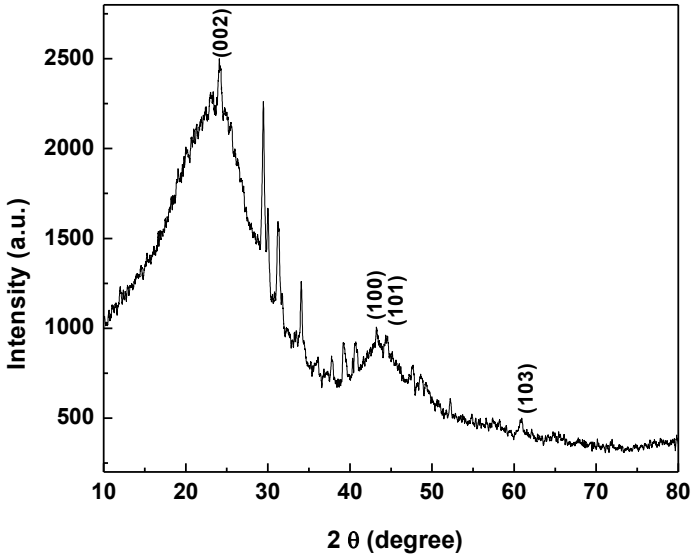

Fig.5.31. XRD pattern of the porous carbon nanomaterials from psyllium seed husk

5.9.3.3. EDS analysis

The chemical compositions of the synthesized materials were analysed using energy dispersive spectral analysis **(Fig.5.32)** which revealed the presence of carbon as the major constituent and traces of oxygen, chlorine, potassium and calcium.

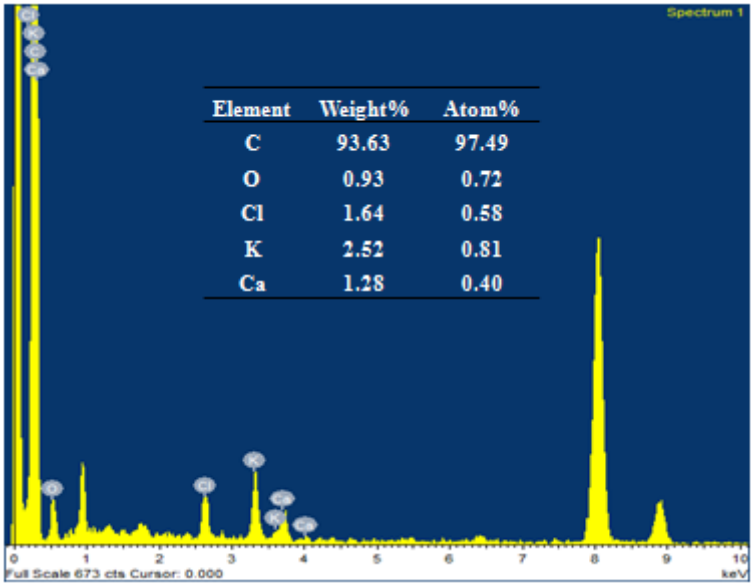

Fig.5.32. EDS spectrum and elemental composition of 'as obtained' porous carbon nanomaterials from psyllium seed husk

5.9.3.4. Photocatalytic activity of porous carbon nanomaterials

The photocatalytic behaviour of the as obtained nanoflakes was evaluated by degradation of methylene blue (MB) solution under visible light irradiation. The decreasing concentration of the MB solution was used to determine the effectiveness of the material as photocatalyst [53, 54]. The intensity of the 665 nm peak of MB solution was monitored to assess the concentration of the MB in solution.

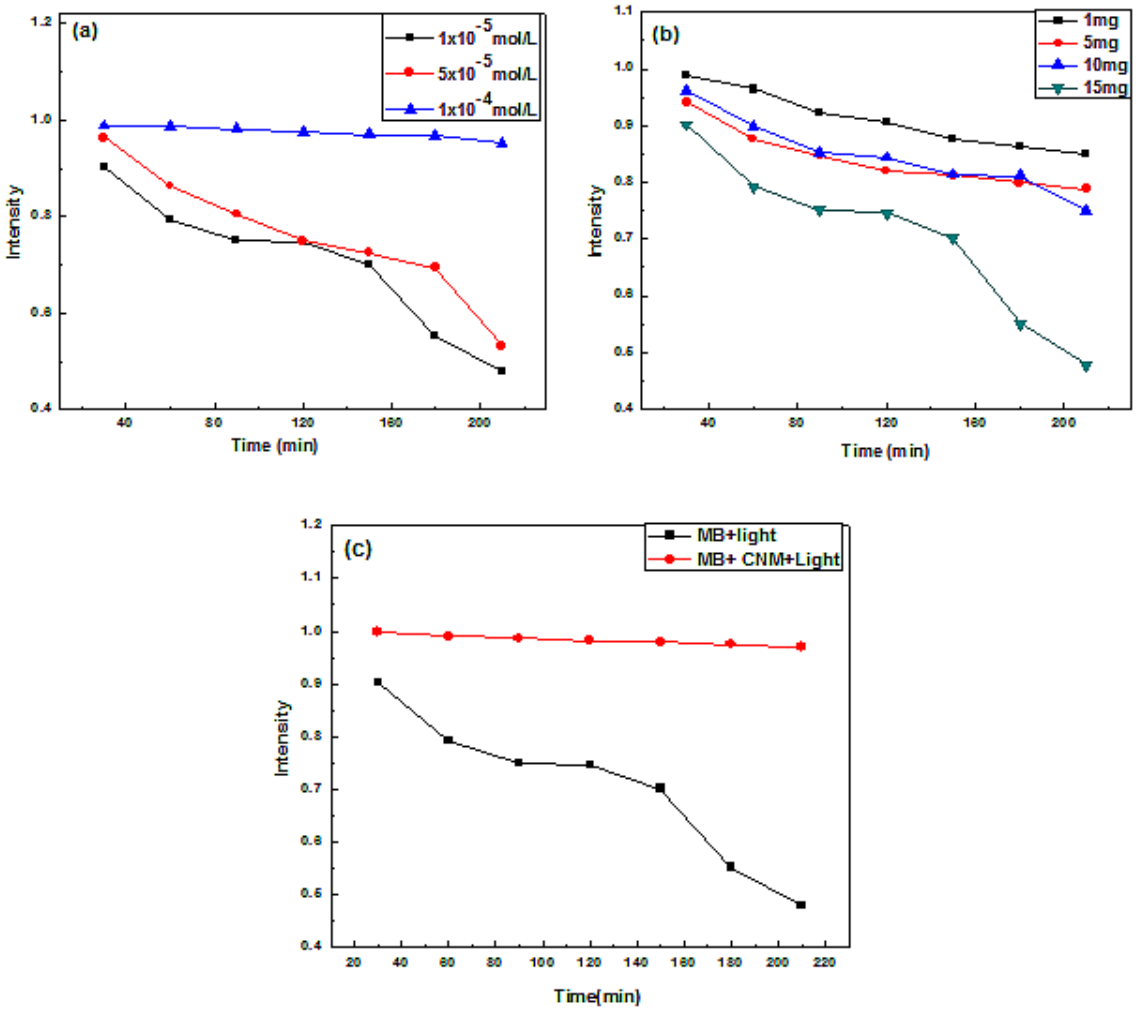

Fig.5.33. (a) Time dependent UV-visible peak intensities at 665 nm of different concentrations of MB solution **(b)** concentration dependent UV-visible intensities at 665 nm of ($1x10^{-5}$ mol/L) with different amounts of nanoflakes material and **(c)** degradation of MB solution ($1x10^{-5}$ mol/L) with visible light treated product and non treated product (MB+CNM)

The photocatalyst (1mg, 5mg, 10mg and 15mg) of as-obtained porous carbon nanomaterial were added into 50mL of MB solution in distilled water of

concentrations $1x10^{-5}$ mol/L, $5x10^{-5}$ mol/L and $1x10^{-4}$mol/L, respectively. After being dispersed in an ultrasonic bath for 5 min, the solutions were stirred for 2 hour in the dark to reach adsorption equilibrium between the catalyst nanoflakes and the solution and then exposed to visible-light irradiation. The samples are taken out at specific time interval and centrifuged to separate the suspended particles. The readings were recorded on a spectrophotometer at an interval of 30, 60, 90, 120, 150, 180 and 210 minutes **(Fig 5.33(a,b)).** It is evident that the nanoflakes alone as such do not exhibit any degradation efficacy in absence of light, but in presence of visible light a marked degradation was noticed **(Fig.5.33(c)).**

5.10. Carbon nanosieve from papaya stems fibre (*Carica papaya*)

5.10.1. Materials

The papaya is the fruit of the plant *Carica papaya*, and is one of the 22 accepted species in the genus *Carica* of the plant family Caricaceae. Papaya plant is grown extensively all over the tropical regions under cultivated farms for its fruits as well as for latex, *papain*, enzyme that found wide applications in the food industry. The ripe fruits are usually eaten raw and 100 g of it provides 43 calories and is a significant source of vitamin C and a moderate source of folate. The stem fibers **(Fig.5.34)** were collected and processed and used as a raw material for the preparation of nanofibres.

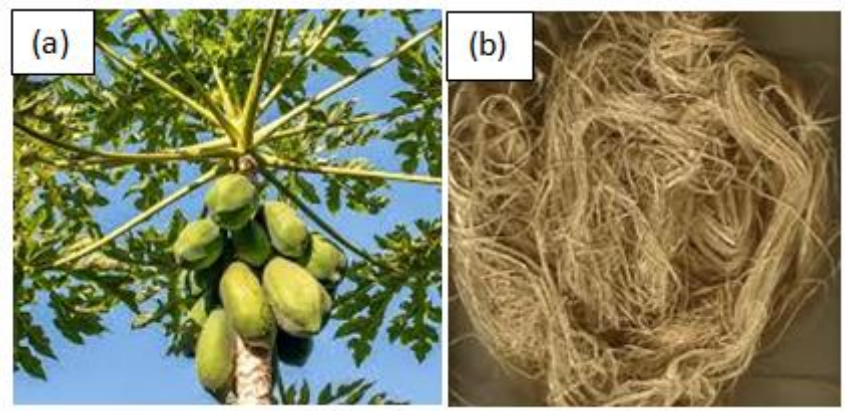

Fig.5.34. Photographs of **(a)** papaya plant **(b)** papaya fibres

5.10.2. Synthesis of carbon nanosieve

Carbon nanosieves were obtained from the washed and dried papaya stems fibres (*Carica papaya*) by pyrolysis in a CVD furnace. A quartz boat loaded with the precursor (~10 g) inserted in a horizontal quartz tube was placed in the furnace. The

tube was initially flushed with argon gas in order to eliminate air from the tube and then purged at a flow rate of 6cm^3/min. The furnace was heated to 800^{0}C at a rate of 7^{0}C/min for 2 hours to complete the process of pyrolysis. The system was then allowed to cool to room temperature under inert condition and the black fibrous materials so formed were taken out from the quartz boat and analyzed as obtained (yield 2.4 g).

5.10.3. Results and discussion

The as-obtained black fibrous material was found to be stable in air for months and can be brought into dispersion in aqueous and organic solvents (methanol, ethanol) under ultrasonication. The yield of the nanomaterial was found to be around ~25% by weight of the initial biomass. The tap density of the synthesised porous carbon nanosieves was found to be 0.47g/cm^3.

5.10.3.1. Scanning electron microscopy

The SEM micrographs of the as obtained carbon nanomaterials **(Fig.5.35)** indicated unique structural features. The material is highly porous with symmetrically organized oval shaped pores of dimension in the range ~2-4µm.

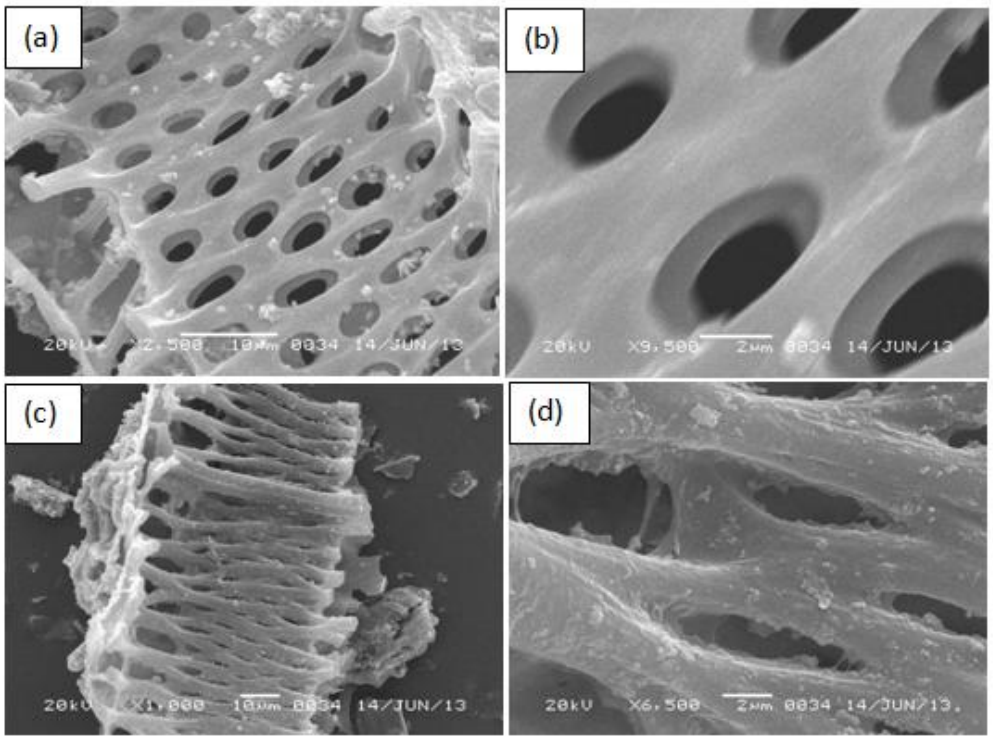

Fig.5.35. (a-d) SEM micrograph of carbon nanosieve from papaya stems fibre

The wall thickness of the nanosieve is found to be ~700 nm. The cross-sectional view revealed that the porous carbon framework is decorated with homoaligned interconnected thread like extensions of length ~ 50μm and cross section ~2μm. It is worth mentioning that the materials with porous textures are at the heart of many applications such as renewable energy storage and generation, reservoirs for electrolyte. Such unique textural characteristic is of great significance for fast charge transport and superior to the solid structure without porosity [56].

5.10.3.2. X-ray diffraction study

The powder XRD pattern of the as-obtained carbon nanosieve (**Fig.5.36**) showed four major Bragg peaks at 2θ = 25.58 , 42.6, 44.51 and 50.96 corresponding to the (002), (100), (101) and(102) planes, respectively of hexagonal graphitic carbon possessing $P6_3/mmc$ space group (JCPDS Card No. 23-0064). The broad nature of these peaks suggests a lesser long range structural order. Interlayer spacing (d=0.33nm) obtained from both HRTEM and Bragg's equation evidences a rather high degree of graphitic character of nanosieve.

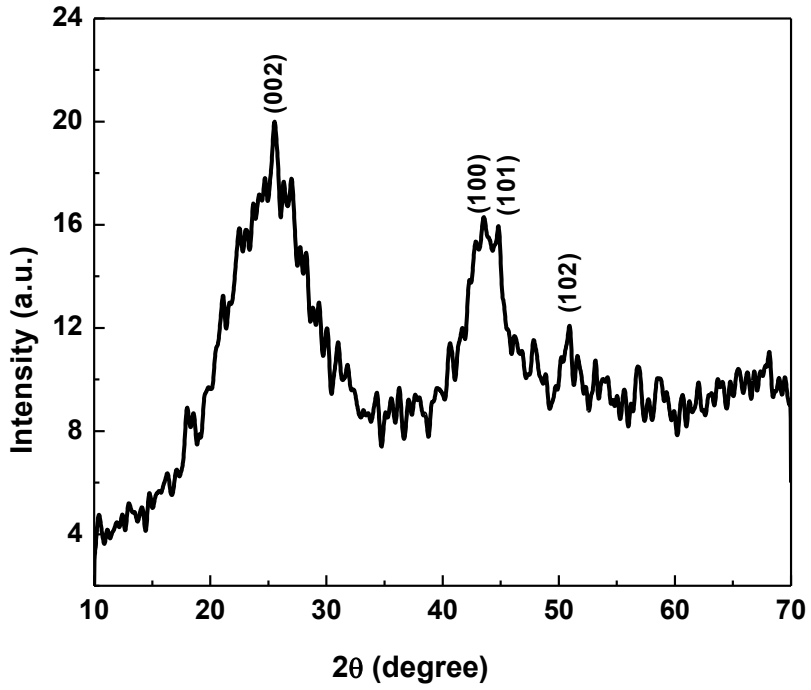

Fig.5.36. XRD pattern of carbon nanosieve from papaya stem fibre

5.11. Carbon nanofibres from seed of *Oroxylum indicum*

5.11.1. Materials

The raw materials used for the synthesis were the seeds of *Oroxylum indicum* plant, locally called honur **(Fig.5.37).** The plant grows wild in the lowland forest, often near villages and rice field. The plant has been claimed to be able to act as an anti-tumour, an antimalarial and antimicrobial. The tall tree develops spectacular, meter-long curved scimitar-like pods. The fruit were collected from Hailakandi, Assam, India, seeds were taken out and washed, sun dried and used as precursor to synthesize nanofibres.

Fig.5.37. Photographs of **(a)** *Oroxylum indicum* plant **(b, c)** *Oroxylum indicum* seeds

5.11.2 Synthesis of carbon nanofibres

The synthesis of carbon nanofibres from seed of *Oroxylum indicum* was carried out by pyrolysis under inert condition. The dried seeds (10g) taken in a quartz boat was heated to 800^0C in a chemical vapour deposition furnace at a rate of 7^0C /min for 2 hours under argon flow rate of $6cm^3$/min to afford a black powder. The yield recorded was 2.8 g.

5.11.3. Results and discussion

5.11.3.1. Scanning electron microscopy

The SEM micrographs **(Fig.5.38)** revealed the presence of fibres of length more than 600μm. The surface of the fibres was found to be shabby. The fibres were seemed to be consisting of layers growing non-uniformly in one dimension via layer by layer mechanism with layer thickness ~15nm.

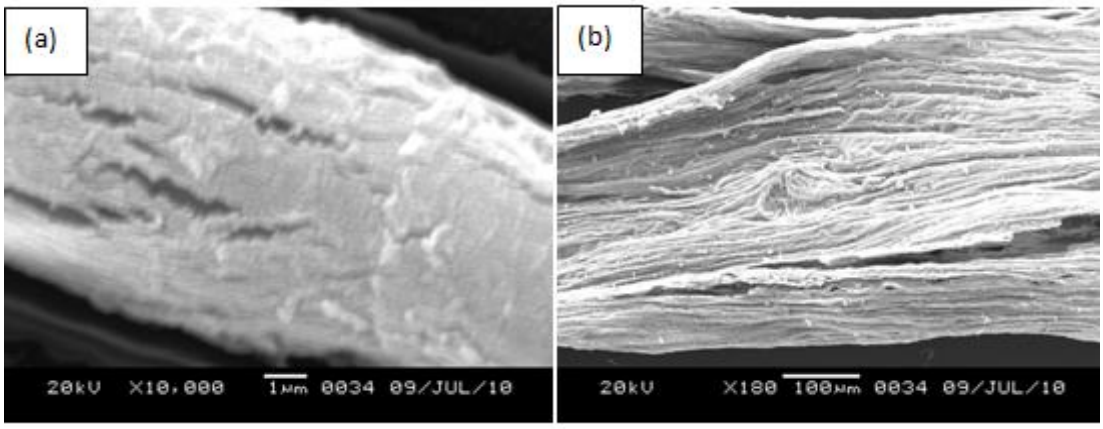

Fig.5.38. (a, b) SEM micrographs of nanofibres from seed of *Oroxylum indicum*

5.11.3.2. Powder X-ray diffraction study

The powder X-ray diffraction pattern was recorded for identification of phases exhibited by the synthesised material. The XRD pattern **(Fig.5.39)** showed the presence of a broad major peak centered at ~25^0 and secondary peaks, ~43^0, ~45^0, ~51^0, ~54^0, ~61^0 related to the (002), (100), (101), (102), (004) and (103) planes of hexagonal graphitic carbon respectively. The diffraction peaks are clearly broad indicating reduced crystallite size and lower degree of graphitization.

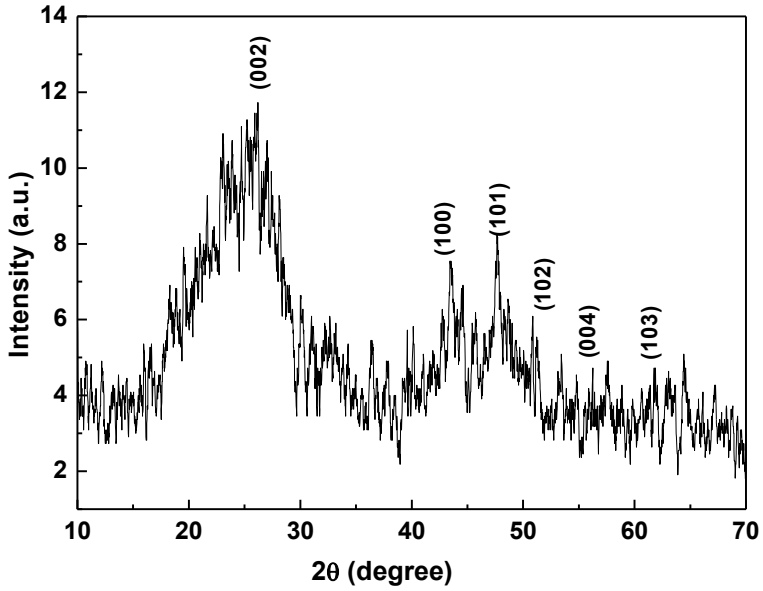

Fig.5.39. XRD pattern of nanofibres from seed of *Oroxylum indicum*

5.12. Carbon nanosheets from colorful papery bracts of *Bougainvillea spectabilis*

5.12.1. Materials

Bougainvillea spectabilis **(Fig.5.40)**, also known as bougainvillea or paper flower, is a species of flowering plant, belongs to Nyctaginaceae family. It has shiny green, slightly hairy leaves and magenta coloured bracts, is an evergreen, climbing woody vine. *Bougainvillea spectabilis* grows as a woody vine or shrub with heart-shaped leaves and thorny, pubescent stems. The flowers are generally small, white, and inconspicuous, highlighted by several brightly coloured modified leaves called bracts**.** It has been reported to have anti-inflammatory, anti-bacterial, anti-viral, anti-tumor, anti-hypercholestrolemic, anti-hyperlipidemic and anti-fertility properties. The plant is widely grown as an ornamental plant and is used for bonsai. Colourful papery bracts of flower of *Bougainvillea spectabilis* are collected from S.S. College, premises, Hailakandi, Assam, India during April to June, 2012. Colorful papery bracts of flower were thoroughly washed, sun dried, crushed and used as precursor to synthesize CNF.

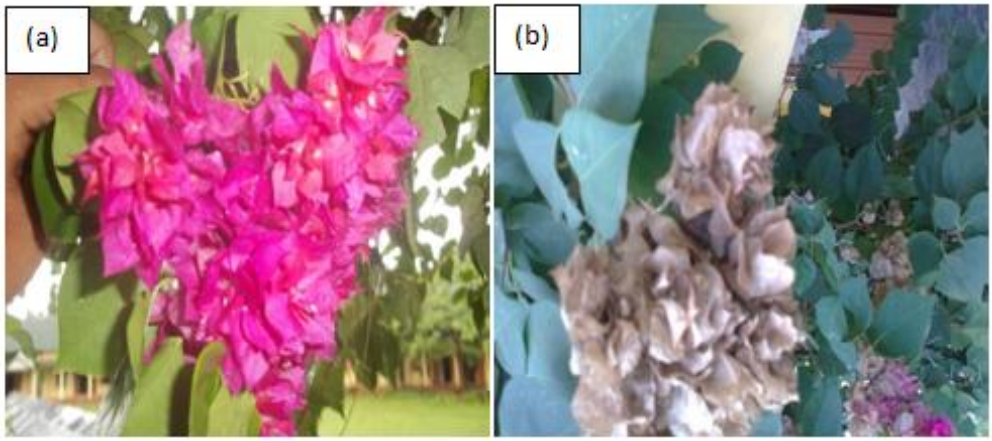

Fig.5.40. Photographs of **(a)** colourful papery bracts **(b)** dried papery bracts of *Bougainvillea spectabilis*

5.12.2. Synthesis of carbon nanosheets

A quartz boat loaded with 10 g of dried, washed papery bracts of *Bougainvillea spectabilis* was kept inside the horizontal quartz tube (1m long with an inner diameter of 25 mm), which was mounted inside a reaction furnace (300 mm long). The outer part of the quartz tube was attached with a water bubbler. The horizontal quartz tube containing quartz boat was first flushed with argon gas in order to eliminate air from the tube. Then the gas was allowed to flow with a flow rate of 6ml/min. Furnace was

then switched on to attain the set temperature of 800^0C at the rate of 7^0C. When the desired temperature is reached, furnace was left on for a set time of 2 hours and then allowed to cool. After cooling the furnace, carbon nanomaterials so formed inside the boat were taken out and then the purified by heating at 400^0C in an open air for half an hour to remove the amorphous carbon and yield was recorded (2.6g).

5.12.3. Results and discussion

The as-obtained black puffy material is air stable for months and can be dispersed in aqueous and organic solvents (methanol, ethanol) under ultrasonication. The yield of the material was found to be around ~25% by weight of the initial biomass. The tap density of the material is found to be 0.374 g/cm^3.

5.12.3.1. Scanning electron microscopy and transmission electron microscopy

The SEM micrographs (**Fig.5.41.**) revealed the presence of nanoflakes of irregular shape with the size ranging from a few to tens of micrometers. The materials were seemed to be consisting of layers with layer thickness ~ 150nm. The surface of the some flakes has been found to be decorated with uniform white patches.

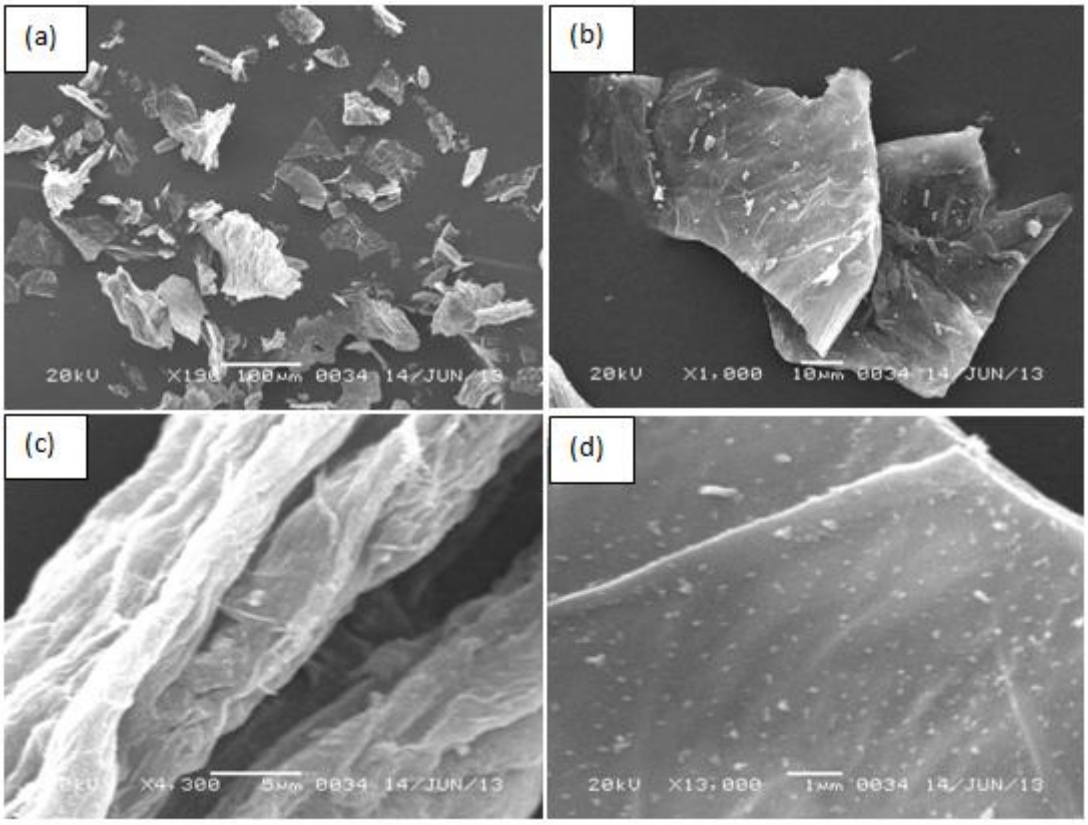

Fig.5.41. (a-d) SEM micrographs of nanosheets from papery bracts of *Bougainvillea spectabilis*

The TEM micrographs **(Fig.5.42)** of the as obtained materials revealed the presence of graphene like sheets with sharp edges stacked together. The thickness of the sheets was found to be ~ 1.4nm. The lattice fringes were not very distinct. The interplanar distance is however calculated to be 0.33 nm which correspond to (002) plane of graphitic carbon. The concentric ring pattern in SAED attested the graphitic nature of the material.

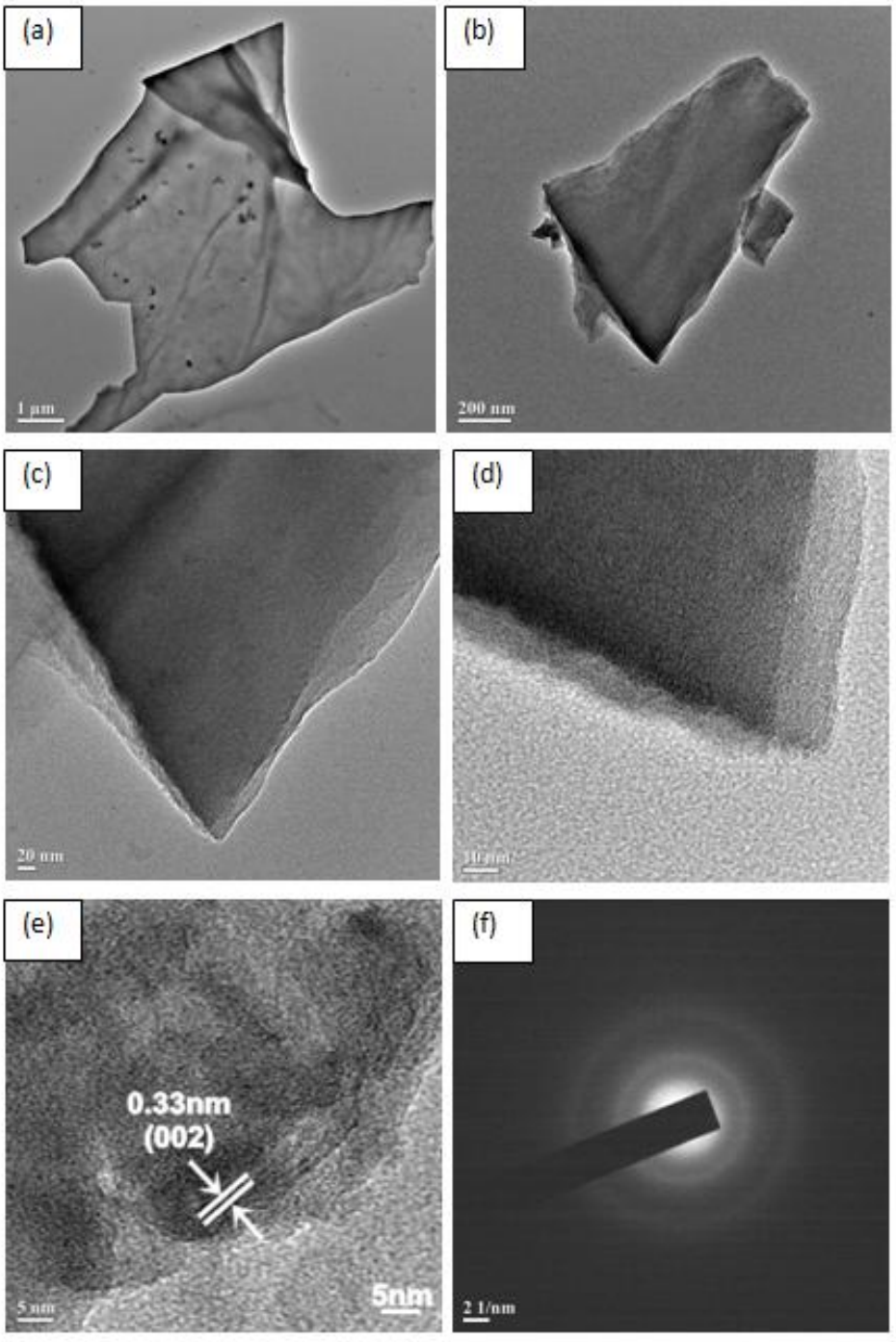

Fig.5.42.(a-d) TEM images **(e)** HRTEM image **(f)** SAED pattern of nanosheets from colorful papery bracts of *Bougainvillea spectabilis*

5.12.3.2. Powder X-ray diffraction study

The powder X-ray diffraction pattern was recorded for identification of phases exhibited by the synthesised material. The XRD pattern**(Fig.5.43)** showed the presence of major peaks centered at ~26^0, ~43^0, ~45^0, ~50^0, ~54^0 , ~61^0 related to the (002), (100), (101), (102), (004) and (103) planes of hexagonal graphitic carbon respectively. The diffraction peaks are clearly broad indicating reduced crystallite size. The average crystallite size for the most intense peak by Debye-Scherrer formula, using a Gaussian fit was found to be 20.86 nm.

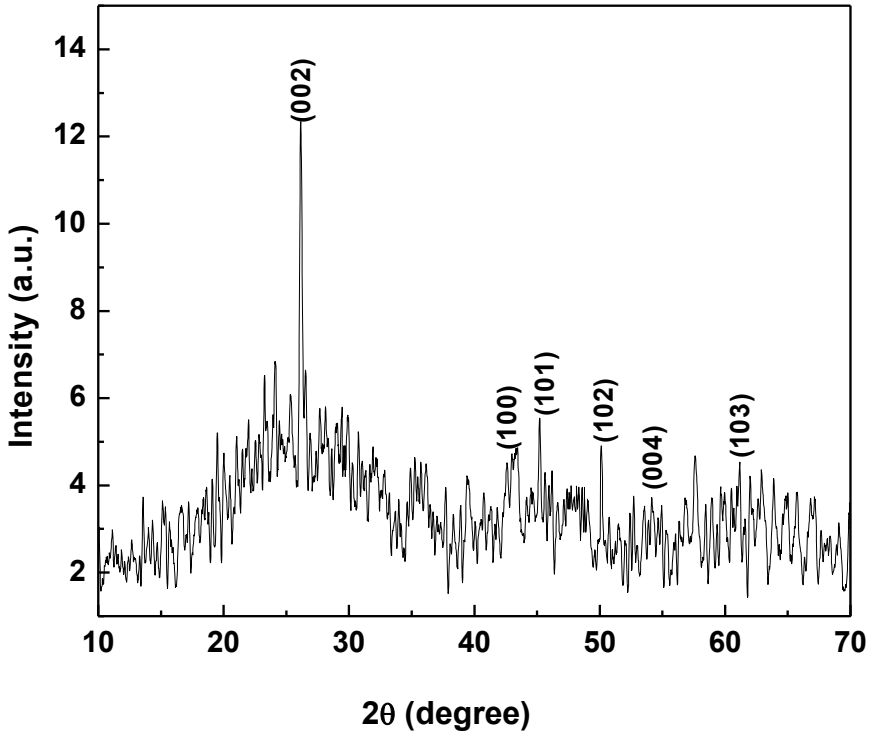

Fig.5.43. XRD pattern of nanosheets from colorful papery bracts of *Bougainvillea spectabilis*

5.13. Carbon nanoflakes from bontula, *Bombax insigne*

5.13.1. Materials

The *Bombax insigne* is commonly known as bontula and belongs to the family bombacaceae. The fruits of *Bombax insigne* were collected from Karimganj College premises of Karimganj, Assam, India during April to June, 2012. The fibres **(Fig.5.44)** taken out from the seeds, washed, sun dried and used as precursor to synthesize carbon nanoflakes.

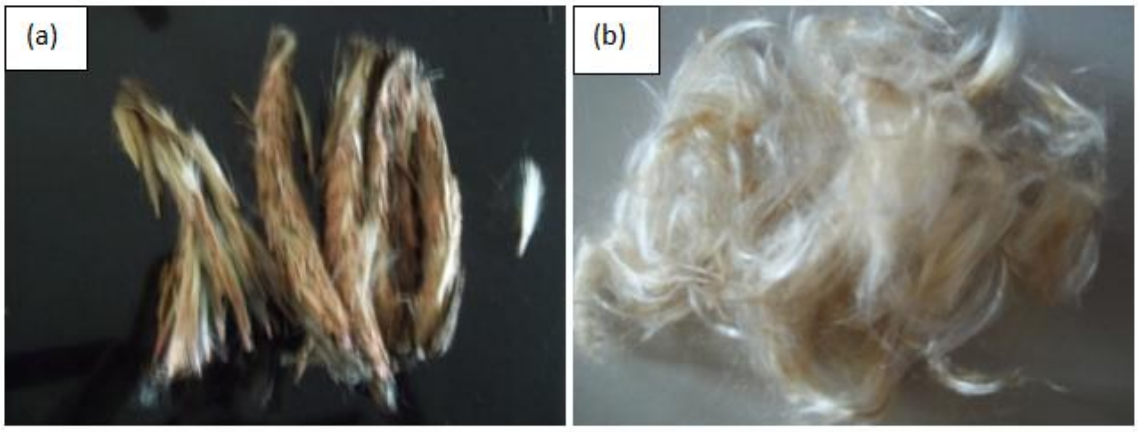

Fig.5.44. (a,b) Photographs of bontula (*Bombax insigne)*fibres

5.13.2. Synthesis of carbon nanofibres

A quartz boat loaded with 10 g of washed, sun dried fibres of *Bombax insigne* was kept inside the horizontal quartz tube (1m long with an inner diameter of 25 mm), which was mounted inside a reaction furnace (300 mm long). The outer part of the quartz tube was attached with a water bubbler. The horizontal quartz tube containing quartz boat was first flushed with argon gas in order to eliminate air from the tube. Then the gas was allowed to flow with a flow rate of 6ml/min. Furnace was then switched on to attain the set temperature of 800^0C at the rate of 7^0C. When the desired temperature is reached, furnace was left on for a set time of 2 hours and then allowed to cool. The as obtained carbon nano materials was collected and yield was recorded (3.2g).

5.13.3. Results and discussion

The as-obtained black puffy materials is air stable for months and can be dispersed in aqueous and organic solvents (methanol, ethanol) under ultrasonication. The yield of the material was found to be around ~30% by weight of the initial biomass. The tap density of the material is found to be 0.374 g/cm^3.

5.13.3.1. Scanning electron microscopy and transmission electron microscopy

The SEM micrographs **(Fig.5.45 (a,b))** indicated the presence of flakes of irregular shape. The thickness of the flakes was found to be ~700nm. The high resolution TEM image **(Fig.5.45(c))** indicated lattice fringes with interplanar distance 0.33 nm which

correspond to (002) plane of graphitic carbon. The concentric ring pattern in SAED attested the graphitic nature of the material.

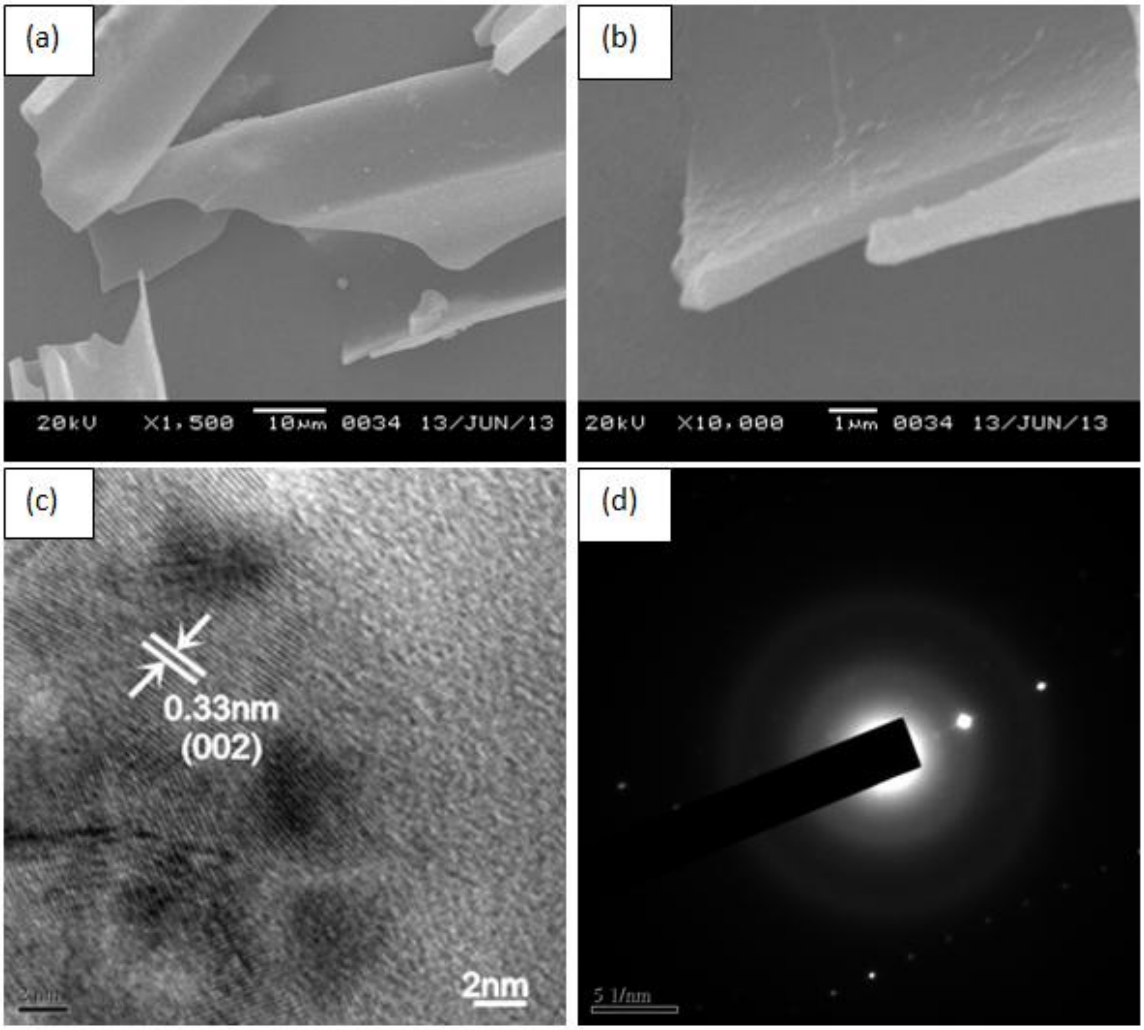

Fig.5.45.(a,b) SEM micrographs **(c)**HRTEM micrograph **(d)** SAED pattern of nanoflakes obtained from bontula

5.13.3.2. EDS analysis

The chemical compositions of the synthesized materials were analysed using energy dispersive spectral analysis **(Fig.5.46)** which revealed the presence of carbon as the major constituent and minor contribution from oxygen and traces of silicon, and potassium.

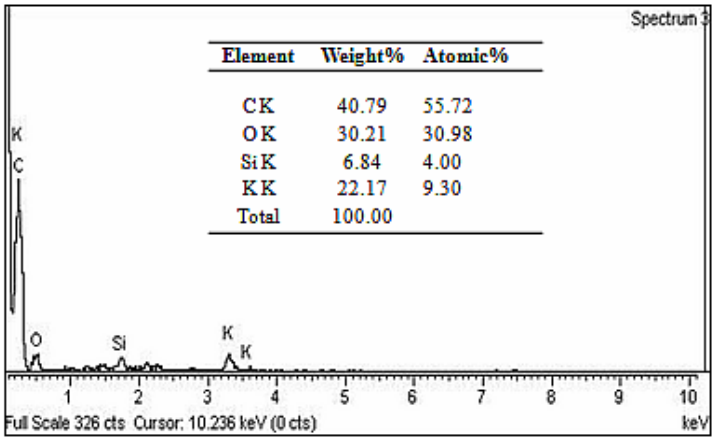

Fig.5.46.EDS and chemical composition of nanoflakes

5.13.3.3. X-ray diffraction study

The powder X-ray diffraction pattern was recorded for identification of phases exhibited by the synthesised material. The XRD pattern **(Fig.5.47)** showed the presence of peak centered at ~24.9^0, ~42.0^0 , ~42.0^0 , ~50.0^0 related to the (002), (100), (101) and (102) planes of hexagonal graphitic carbon respectively. The diffraction peaks indicates low crystallinity.

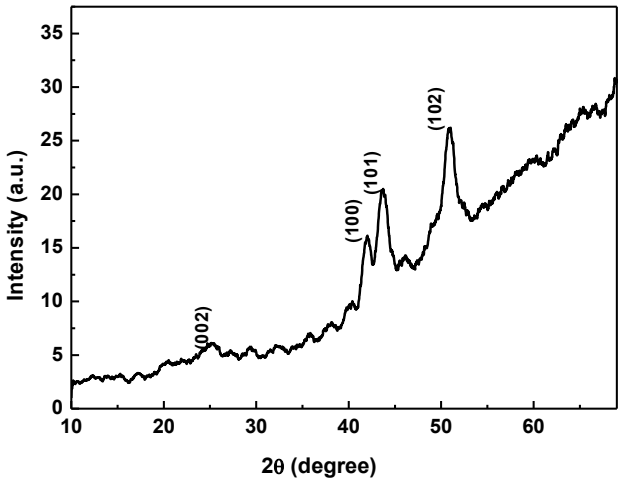

Fig.5.47. XRD pattern of nanoflakes obtained from bontula

5.14. Carbon nano flakes from seed coat of spinach (*Spinacia oleracea)*

5.14.1. Materials

Spinacia oleracea **(Fig.5.48)** is commonly known as spinach and locally called *thunga or tak palong*. It is an edible flowering plant in the family Amaranthaceae. The seeds and seed coats were collected from home vegetable garden at Silchar, Assam,

India. The soft seed coat were taken out, thoroughly washed, sun dried, chopped and used as precursor to synthesize carbon nanoflakes.

Fig.5.48. Photographs of **(a)** spinach plant **(b)** spinach seed coat

5.14.2. Synthesis carbon nanoflakes

Carbon nanoflakes were produced from the washed and dried seed coat of *Spinacia oleracea* by pyrolysis in a CVD furnace. A quartz boat loaded with the precursor (~10 g) inserted in a horizontal quartz tube was placed in the furnace. The tube was initially flushed with argon gas in order to eliminate air from the tube and then purged at a flow rate of 6cm^3/min. The furnace was heated to 800 ^{0}C at a rate of 7 ^{0}C per minute for 2 hours to complete the process of pyrolysis. The system was then allowed to cool to room temperature under inert condition and the black puffy materials so formed were taken out from the quartz boat and analyzed as obtained (yield 2.4 g).

5.14.3. Results and discussion

The as-obtained black puffy material is found to be stable in air for months and can be dispersed in aqueous and organic solvents (methanol, ethanol) under ultrasonication. The yield of the nanomaterial was found to be around ~25% by weight of the initial biomass. The tap density of the synthesised carbon nanoflake was found to be 0.47g/cm^3.

5.14.3.1. Scanning electron microscopy

The SEM micrographs of the as obtained carbon nanomaterials were presented in **Fig.5.49.** The images indicated unique structural features**.** The carbon nanomaterials showed wavy glacier patterned flakes of length more than 220μm. The flakes are consisting of systematic layers with layer thickness around 30nm.

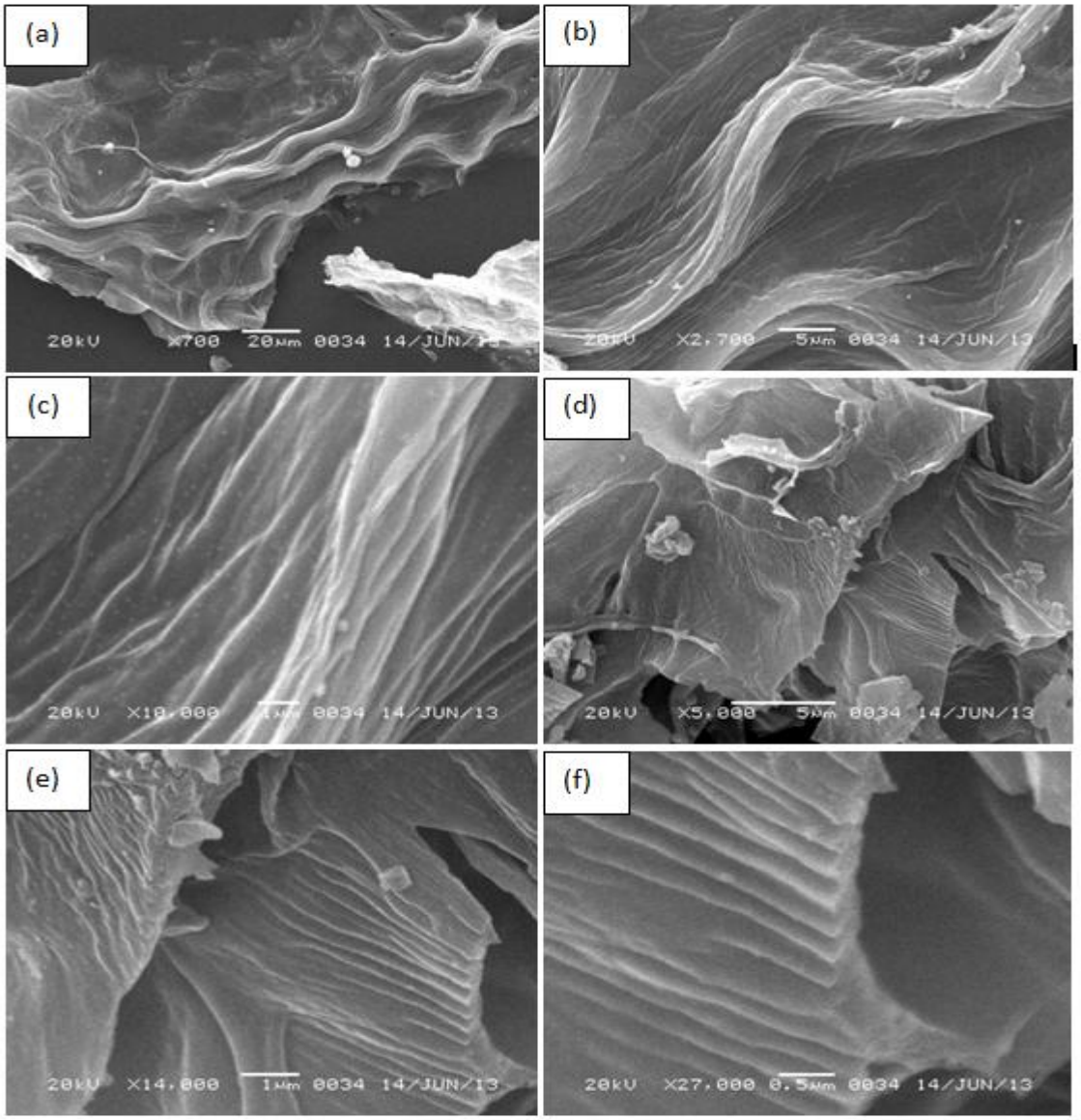

Fig.5.49. (a-f) SEM micrographs of nano flakes from seed coat of spinach

5.14.3.2. Powder X-ray diffraction study

The powder X-ray diffraction pattern was recorded for identification of phases exhibited by the synthesised material. The XRD pattern **(Fig.5.50)** showed the presence of broad major peaks centered at ~24.6^0 and ~44.1^0 and secondary peaks at ~51^0, ~54^0 , ~59^0 related to the (002), (101), (102), (004) and (103) planes of hexagonal graphitic carbon respectively. The diffraction peaks are clearly broad indicating reduced crystallite size. The average crystallite size for the most intense peak by Debye-Scherrer formula, using a Gaussian fit was found to be 11.9 nm.

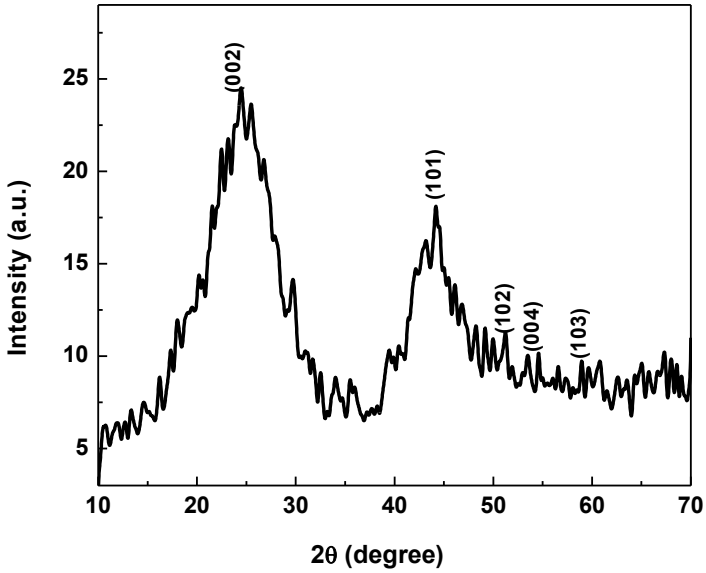

Fig.5.50. XRD pattern of nano flakes from seed coat of spinach

5.15. Carbon nanofibres from betel nut (*Areca catechu*) fibres

5.15.1. Materials

The areca nut, locally called *supari* **(Fig.5.51)**, is the seed of the areca palm (*Areca catechu*), which grows in much of the tropical Pacific, Asia, and parts of east Africa. It is commonly referred to as betel nut, as it is often chewed wrapped in betel leaves (paan). Betel nut's medical use is limited, and long-term negative reactions to betel quid chewing are well known. A decrease in positive symptoms among men with schizophrenia was attributed to betel nut consumption. The seeds were collected from the villages of Hailakandi, Assam, India. The fibres were scrabbled up, washed, dried, chopped and used as precursor to synthesize nanofibres.

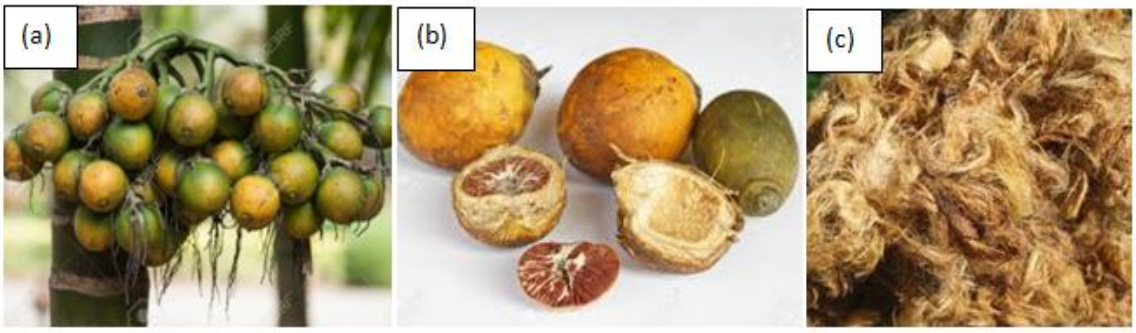

Fig.5.51. Photographs of **(a, b)** betel nut**(c)** betel nut fibre

5.15.2 Synthesis of carbon nanofibres

Carbon nanofibres were produced from the washed and dried fibres of betel nut (*Areca catechu*) by pyrolysis in a CVD furnace. A quartz boat loaded with the precursor (~10 g) inserted in a horizontal quartz tube was placed in the furnace. The tube was initially flushed with argon gas in order to eliminate air from the tube and then purged at a flow rate of $6cm^3$/min. The furnace was heated to 800^0 C at a rate of 7^0C /min for2 hours to complete the process of pyrolysis. The system was then allowed to cool to room temperature under inert condition and the black fibrous materials so formed were taken out from the quartz boat and analyzed (yield 2.7g).

5.15.3. Results and discussion

The as-obtained black fibrous material is found to be stable in air for months and can be dispersed in aqueous and organic solvents (methanol, ethanol) under ultrasonication. The yield of the nanomaterial was found to be around ~25% by weight of the initial biomass. The tap density of the synthesised carbon nanofibre was found to be $0.49g/cm^3$.

5.15.3.1. Scanning electron microscopy and transmission electron microscopy

The SEM micrographs **(Fig.5.52)** showed the presence of millimeter long carbon nanofibres with unique surface texture. The length of the fibre is found to be more than 1.8 mm. Fibres are having some depressions on its surface at almost uniform distance apart along its length. The diameter of the shell is approximately 9µm, containing clusters of beads of irregular shape. The size of the beads are found to be in the range of 500-700nm. It is worth mentioning that the palmyra fibre on pyrolysis under similar conditions yielded similar textures (section **5.2.3.1.**).

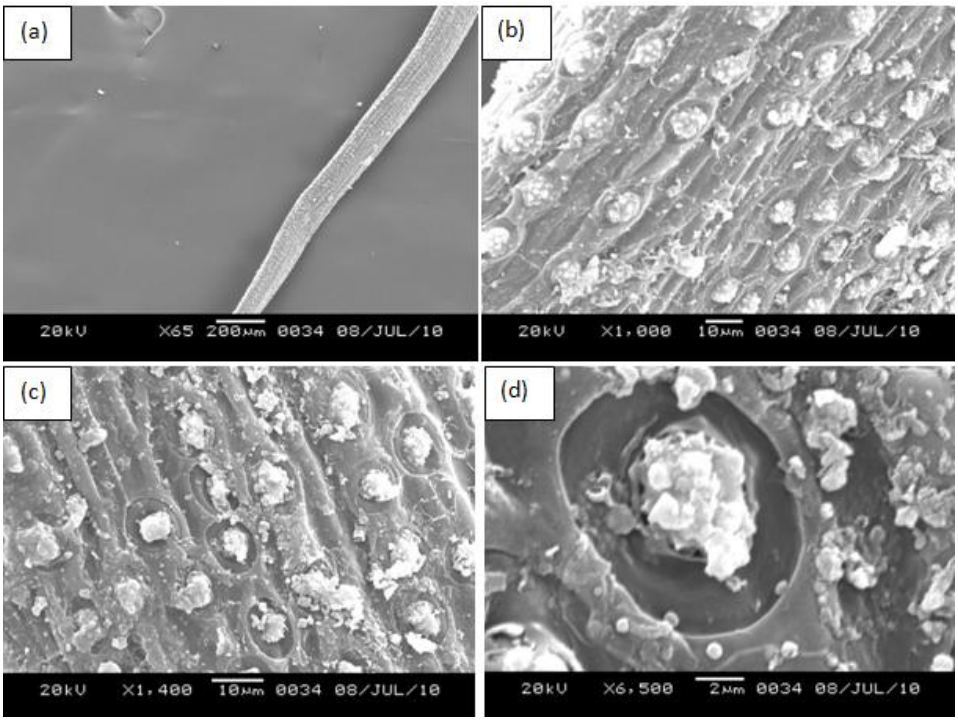

Fig.5.52. (a-d) SEM micrographs of carbon nanofibres from betel nut fibres

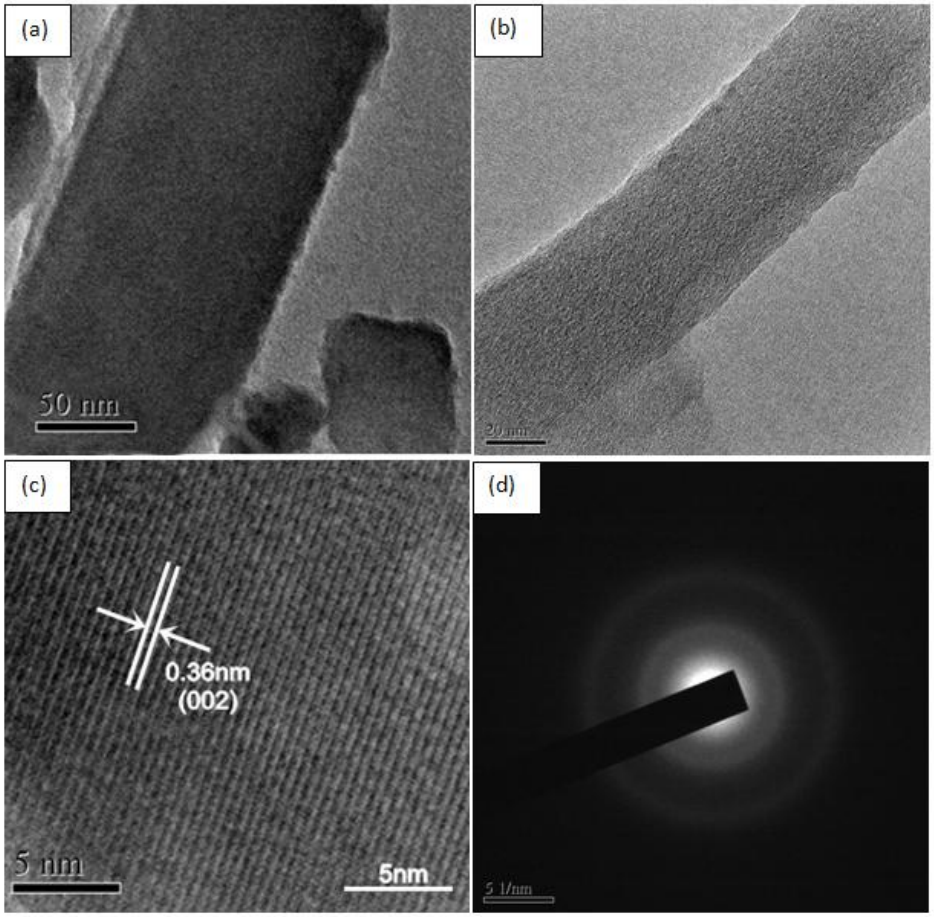

Fig.5.53.(a,b) TEM micrographs **(c)**HRTEM micrograph**(d)**SAED pattern of nanofibres

The TEM micrographs **(Fig.5.53)** also displayed the nanofibres. The size of the fibre was around 60-70 nm. The high resolution TEM image of the internal structure revealed the inter layer distance ~0.36 nm which resembles (002) plane of graphitic carbon. The SAED pattern showed concentric rings indicating polycrystalline nature of the as- obtained carbon nanofibres.

5.15.3.2. Powder X-ray diffraction study

The powder X-ray diffraction pattern was recorded for identification of phases exhibited by the synthesised material. The XRD pattern **(Fig.5.54)** showed the presence of a broad major peak centered at ~26^0 and secondary peaks ~44^0, ~53^0 related to the (002), (101) and (004) planes of hexagonal graphitic carbon respectively. The diffraction peaks are clearly broad indicating reduced crystallite size. The average crystallite size for the most intense peak by Debye-Scherrer formula, using a Gaussian fit was found to be 17.84nm.

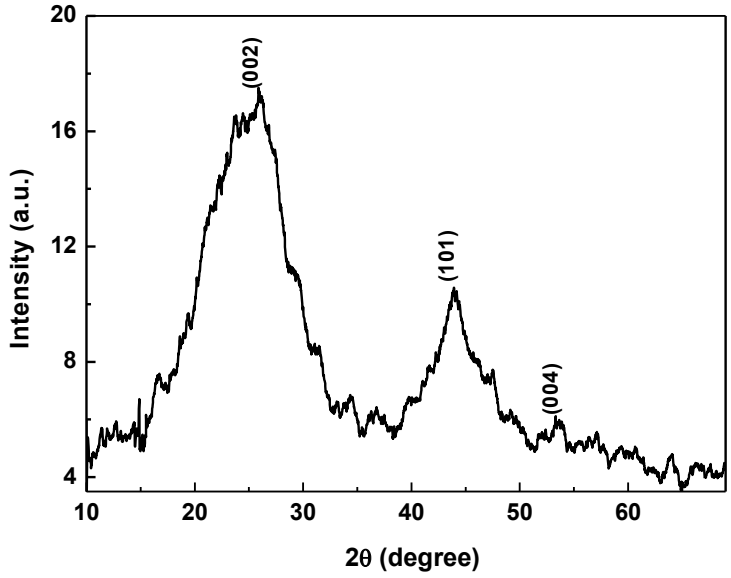

Fig.5.54. XRD pattern of carbon nanofibres from betel nut fibres

References

[1] Kroto, H. W., Heath, J. R., O'Brien, S. C., Curl, R. F., & Smalley, R. E. *Nature*, 1985, **318**, 162.

[2] Bandaru, P. R. *J. Nanosci. Nanotechnol.*, 2007, 7, 1239.

[3] Bernholc, J., Brenner, D., Buongiorno Nardelli, M., Meunier, V., & Roland, C. *Annu. Rev. Mater. Res.*, 2002, **32**, 347.

[4] Frackowiak, E., & Beguin, F. *Carbon*, 2002, **40**, 1775.

[5] Frackowiak, E., & Beguin, F. *Carbon*, 2001, **39**, 937.

[6] Khan, Z. H., & Husain, M. *Indian J. Eng. Mater. S.*, 2005, **12**, 529.

[7] Jang, H. S., Lee, H. R., & Kim, D. H. *Thin Solid Films*, 2006, **500**, 124.

[8] Abellan, G., Coronado, E., Marti-Gastaldo, C., Ribera, A., & Sanchez-Royo, J. F. *Chem. Sci.*, 2012, **3**, 1481.

[9] Jaszczak, J. A., Robinson, G. W., Dimovski, S., & Gogotsi, Y. *Carbon*, 2003, **41**, 2085.

[10] Zhu, S., & Xu, G. *Nanoscale*, 2010, **2**, 2538.

[11] Sharon, M., & Sharon, M. *Carbon Lett.*, 2012, **13**, 161.

[12] Joo, S. H., Choi, S. J., Oh, I., Kwak, J., Liu, Z., Terasaki, O., & Ryoo, R. *Nature*, 2001, **412**, 169.

[13] Auer, E., Freund, A., Pietsch, J., & Tacke, T. *Appl. Catal., A.*, 1998, **173**, 259.

[14] Park, G. G., Yang, T. H., Yoon, Y. G., Lee, W. Y., & Kim, C. S. *Int. J. Hydrogen Energy*, 2003, **28**, 645.

[15] Guha, A., Lu, W., Zawodzinski, T. A., & Schiraldi, D. A. *Carbon*, 2007, **45**, 1506.

[16] Lu, C., & Chiu, H. *Chem. Eng. Sci.*, 2006, **61**, 1138.

[17] Gomez-Serrano, V., Macias-Garcia, A., Espinosa-Mansilla, A., & Valenzuela-Calahorro, C. *Water Res.*, 1998, **32**, 1.

[18] Kaneko, K., & Imai, J. *Carbon*, 1989, **27**, 954.

[19] Bekyarova, E., Murata, K., Yudasaka, M., Kasuya, D., Iijima, S., Tanaka, H., & Kaneko, K. *J. Phys. Chem. B*, 2003, **107**, 4681.

[20] Bigsby, R. J. A., Rider, R. J., & Blount, G. N. *Proc. Inst. Mech. Eng. H.*, 1998, **212**, 373.

[21] Ye, C., Gong, Q. M., Lu, F. P., & Liang, J. *Sep. Purif. Technol.*, 2007, **58**, 2.

[22] Greiner, A., & Wendorff, J. H. *Angew. Chem. Int. Ed. Engl.*, 2007, **46**, 5670.

[23] Shen, Y., Yan, L., Song, H., Yang, J., Yang, G., Chen, X., & Yang, S. *Angew. Chem. Int. Ed. Engl.*, 2012, **51**, 12202.

[24] Hsu, W. K., Hare, J. P., Terrones, M., Kroto, H. W., Walton, D. R., & Harris, P. J. *Nature*, 1995, **377**, 687.

[25] Ren, J., Li, F. F., Lau, J., González-Urbina, L., & Licht, S. *Nano Lett.*, 2015, **15**, 6142.

[26] Vander Wal, R. L., & Hall, L. J. *Chem. Phys. Lett.*, 2001, **349**, 178.

[27] Mahammadunnisa, S., Reddy, E. L., Ray, D., Subrahmanyam, C., & Whitehead, J. C. *Int. J. Green. H. Gas Con.*, 2013, **16**, 361.

[28] Lallave, M., Bedia, J., Ruiz-Rosas, R., Rodríguez-Mirasol, J., Cordero, T., Otero, J. C., & Loscertales, I. G. *Adv. Mater.*, 2007, **19**, 4292.

[29] Bhardwaj, S., Jaybhaye, S., Sharon, M., Sathiyamoorthy, D., Dasgupta, K., Jagadale, P., & Soga, T. *Asian J. Exp. Sci.*, 2008, **22**, 89.

[30] Bhardwaj, S., Sharon, M., Ishihara, T., Jayabhaye, S., Afre, R., Soga, T., & Sharon, M. *Carbon Lett.*, 2007, **8**, 285.

[31] Jagadale, P., Sharon, M., Sharon, M., & Kalita, G. *Synth. React. Inorg. Metal-Org. Nano-Met. Chem.*, 2007, **37**, 467.

[32] Kshirsagar, D. E., Puri, V., Sharon, M., & Sharon, M. *Carbon Lett.*, 2006, **7**, 245.

[33] Zaghib, K., Tatsumi, K., Abe, H., Ohsaki, T., Sawada, Y., & Higuchi, S. *J. Electrochem. Soc.*, 1998, **145**, 210.

[34] Chambers, A., Park, C., Baker, R. T. K., & Rodriguez, N. M. *J. Phys. Chem. B*, 1998, **102**, 4253.

[35] Pradhan, D., Sharon, M., Kumar, M., & Ando, Y. *J. Nanosci. Nanotechnol.*, 2007, **7**, 1034.

[36] Hudnut, S. W., & Chung, D. D. L. *Carbon*, 1995, **33**, 1627.

[37] Zou, G., Zhang, D., Dong, C., Li, H., Xiong, K., Fei, L., & Qian, Y. *Carbon*, 2006, 44, 828.

[38] Sevilla, M., & Fuertes, A. B. *Chem. Phys. Lett.*, 2010, **490**, 63.

[39] Kshirsagar, D. E., Puri, V., Sharon, M., & Sharon, M. *Carbon Lett.*, 2006, **7**, 245.

[40] Bhardwaj, S., Sharon, M., Ishihara, T., Jayabhaye, S., Afre, R., Soga, T., & Sharon, M. *Carbon Lett.*, 2007, **8**, 285.

[41] Khairnar, V., Jaybhaye, S., Hu, C. C., Afre, R., Soga, T., Sharon, M., & Sharon, M. *Carbon Lett.*, 2008, **9**, 188.

[42] Ghosh, P. K. *Indian J. Biochem. Biophys*, 2000, **37**, 273.

[43] Soppimath, K. S., Aminabhavi, T. M., Kulkarni, A. R., & Rudzinski, W. E. *J. Control. Rel.* 2001, **70**, 1.

[44] Pantarotto, D., Partidos, C. D., Hoebeke, J., Brown, F., Kramer, E. D., Briand, J. P., Muller, S., Prato, M. & Bianco, A. *Chem. Biol.*, 2003, **10**, 961.

[45] Lin, Y., Taylor, S., Li, H., Fernando, K. S., Qu, L., Wang, W., & Sun, Y. P. *J. Mater. Chem.*, 2004, **14**, 527.

[46] Parihar, S., Sharon, M., & Sharon, M. *Synth. React. Inorg. Metal-Org. nano-Met.l Chem.*, 2006, **36**, 107.

[47] Serpen, A., Capuano, E., Fogliano, V., & Gokmen, V. *J. Agric. Food Chem.*, 2007, **55**, 7676.

[48] Naik, G. H., Priyadarsini, K. I., Satav, J. G., Banavalikar, M. M., Sohoni, D. P., Biyani, M. K., & Mohan, H. Phytochemistry, 2003, **63**,97.

[49] Ruan, C., Ai, K., & Lu, L. *RSC Advances*, 2014, **4**, 30887.

[50] Schuler, T., & Tremel, W. *Chem. Commun.*, 2011, **47**, 5208.

[51] Theivasanthi, T., & Alagar, M., *Nano Biomed. Eng.*, 2012, **4,** 58.

[52] Zhang, N., Zhang, Y., & Xu, Y. J. *Nanoscale*, 2012, **4**, 5792.

[53] Chang, T., Li, Z., Yun, G., Jia, Y., & Yang, H. *Nano-Micro Lett.*, 2013, **5**, 163.

[54] Woan, K., Pyrgiotakis, G., & Sigmund, W. *Adv. Mater.*, 2009, **21**, 2233.

[55] Ruan, C., Ai, K., & Lu, L. *RSC Advances*, 2014, **4**, 30887.

[56] Lee, J., Kim, J., & Hyeon, T, *Adv. Mater.*, 2006, **18**, 2073.